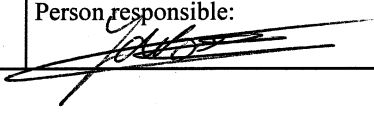


The report is based on a cooperation project of:



NGU Report 2009.069

Thermogeology in the Oslo region and
Kristiansand – Results from thermal response
tests (TRT) with and without artificially induced
groundwater flow

Report no.: 2009.069		ISSN 0800-3416	Grading: Open
Title: Thermogeology in the Oslo region and Kristiansand – Results from thermal response tests (TRT) with and without artificially induced groundwater flow			
Authors: Heiko T. Liebel, Kilian Huber, Bjørn Frengstad, Randi K. Ramstad, Bjarge Brattli		Client: NGU and NTNU	
County: Akershus, Buskerud, Oppland, Oslo, Vest-Agder, Østfold		Commune: Bærum, Fredrikstad, Kristiansand, Oslo, Modum, Rælingen, Vestre Toten	
Map-sheet name (M=1:250.000)		Map-sheet no. and -name (M=1:50.000)	
Deposit name and grid-reference:		Number of pages: 57	Price (NOK):
		Map enclosures:	
Fieldwork carried out: June – August 2009	Date of report: 16.12.2009	Project no.: 328700	Person responsible: 
Summary: <p>Thermal response tests (TRT) are widely used to measure the effective thermal conductivity and borehole resistance in a well. The gained data serve as the basis for the dimensioning of larger ground-source heat-pump installations with closed loop systems. The influence of groundwater flow on a TRT in fractured aquifers is not well understood. An attempt to quantify the influence of groundwater was done by pumping of groundwater from a nearby well during the TRT. The results were compared to a TRT in the same well without pumping. The effect of the groundwater flow is shown indirectly by the higher measured thermal conductivity and directly through the comparison of temperature profiles before and four hours after the TRT.</p> <p>Furthermore, seven TRTs were performed in the geologically diverse Oslo region and data collected from TRTs that were carried out by other companies. The data is compared with lab measured thermal conductivities from rock cores. Thermal conductivities measured by TRTs are by trend higher than those from rock cores but the dataset is still too limited for a statistical quantification of the add-on. The data of this investigation indicate that thermal conductivity maps based on surface rock core samples cannot replace TRTs as there are too many variables linked to both measurements (TRT: presence of groundwater, several geological layers with varying mineral content along the well, thermal anisotropy etc.; rock core samples: punctual measurement, partly drained in the lab, thermal anisotropy etc.). Based on this study it is recommended to take standardized temperature profiles before and four hours after a TRT to get information about varying thermal properties of the ground along the well and about the presence/absence of groundwater flow.</p>			
Keywords: Thermal response test	Temperature profile	Oslo region	
Bryn	Groundwater	Ground-source heat	
FEFLOW	TRT	Heat flow	

CONTENTS

1. INTRODUCTION	1
2. METHODS, EQUIPMENT AND INVESTIGATION SITES	4
2.1 BRYN	6
2.1.1 Site description	6
2.1.2 Geology	7
2.1.3 Hydrogeology	9
2.1.4 Thermogeology	11
2.2 OSLO REGION	12
2.2.1 Fredrikstad	14
2.2.2 Kristiansand	14
2.2.3 Lysaker	16
2.2.4 Modum	16
2.2.5 Nordstrand	17
2.2.6 Raufoss	18
2.2.7 Smestad	18
3. RESULTS AND DISCUSSION	19
3.1 BRYN	19
3.1.1 Thermogeology	19
3.1.2 Temperature profiles	22
3.2 OSLO REGION	24
3.2.1 Thermogeology	24
3.2.2 Temperature profiles	30
a) Undisturbed temperature profiles.....	30
b) Temperature profiles after TRTs.....	32
c) Delta temperature profiles	34
d) Geothermal gradients	36
e) Influence of buildings.....	38
4. GLOBAL EVALUATION	40
4.1 BRYN	40
4.2 OSLO REGION	41
4.3 FURTHER WORK AND RECOMMENDATIONS	42
5. CONCLUSIONS	43
6. ACKNOWLEDGMENTS	44
7. LITERATURE	45
APPENDIX A: TRT data, Oslo region	50
APPENDIX B: Borehole resistance, Bryn	57

FIGURES

Fig. 1.1: Relative greenhouse gas emissions in the year 2000 by source (Stern, 2006 mod.).....	2
Fig. 2.1: TRT rig during operation at Kristiansand Sørlandssenter.....	5
Fig. 2.2: Temperature logging equipment.....	5
Fig. 2.3: Map of the well field at Bryn, Bærum municipality (Ramstad 2004).....	7
Fig. 2.4: Ripple marks on bedding surface and Fisher fracture stereogram, Bryn.....	8
Fig. 2.5: a) View towards NE along the river valley of Lomma. b) fracture fillings, Bryn.....	8
Fig. 2.6: Recovery from steady-state conditions at borehole 2, Bryn.....	10
Fig. 2.7: Parallel drawdown of the groundwater level in all boreholes of the well field in Bryn.....	10
Fig. 2.8: TRT setup at borehole 3 for the test with pumping of groundwater, Bryn.....	11
Fig. 2.9: Overview of locations where TRTs were performed in the Oslo region.....	12
Fig. 2.10: Geological outcrops at the investigation sites in the Oslo region.....	13
Fig. 2.11: Sinistral normal fault forming open fracture planes, Kristiansand.....	15
Fig. 2.12: Cataclastic contact between two moved layers, Kristiansand.....	15
Fig. 2.13: Equal area stereonet showing the poles to open fractures, Kristiansand.....	16
Fig. 2.14: Felsic pegmatite dyke, Nordstrand.....	17
Fig. 2.15: Dark red siltstone with coarse bioturbation burrows, Raufoss.....	18
Fig. 2.16: Banded gneisses and migmatitic gneisses, Smestad.....	19
Fig. 3.1: TRT with pumping of groundwater from borehole, Bryn.....	20
Fig. 3.2: TRT without pumping of groundwater, Bryn.....	20
Fig. 3.3: Temperature profiles before and after both TRTs, Bryn.....	22
Fig. 3.4: Temperature profiles corrected for the elevated “undisturbed” ground temperature before TRT2.....	23
Fig. 3.5: Thermal conductivity map of the Oslo region.....	25
Fig. 3.6: Median thermal conductivity (λ_{Median}) of the according geological unit <i>versus</i> effective thermal conductivity (λ_{eff}).....	26
Fig. 3.7: Effective thermal conductivity for igneous, metamorphic and sedimentary rock.....	27
Fig. 3.8: Statistical variation of the thermal conductivity in four geological units of the Oslo region.....	28
Fig. 3.9: Temperature profile, thermal gradients and heat flow (borehole depth: 200 m), Fredrikstad.....	31
Fig. 3.10: Temperature profile, geothermal gradient and heat flow (borehole depth: 80 – 200 m), Fredrikstad.....	32
Fig. 3.11: Heat flow at all sites.....	33
Fig. 3.12: Delta temperature profiles: Smestad, Raufoss, Fredrikstad and Modum.....	35

Fig. 3.13: Temperature profiles according to their elevation, all sites.....	36
Fig. 3.14: Position of boreholes at "Nordstrand videregående skole".....	38
Fig. 3.15: Temperature profiles and heat flow in four boreholes at Nordstrand.....	39
Fig. 3.16: Simulated heat plume below Nordstrand school.....	39

Figures of the APPENDIX:

Fig. A1: TRT data, Fredrikstad.....	50
Fig. A2: Borehole resistance, Fredrikstad.....	50
Fig. A3: TRT data, Kristiansand.....	51
Fig. A4: Borehole resistance, Kristiansand.....	51
Fig. A5: TRT data, Lysaker.....	52
Fig. A6: Borehole resistance, Lysaker.....	52
Fig. A7: TRT data, Modum.....	53
Fig. A8: Borehole resistance, Modum.....	53
Fig. A9: TRT data, Nordstrand.....	54
Fig. A10: Borehole resistance, Nordstrand.....	54
Fig. A11: TRT data, Raufoss.....	55
Fig. A12: Borehole resistance, Raufoss.....	55
Fig. A13: TRT data, Smestad.....	56
Fig. A14: Borehole resistance, Smestad.....	56
Fig. B1: Borehole resistance at Bryn during TRT2 (without pumping of groundwater).....	57
Fig. B2: Borehole resistance at Bryn during TRT1 (with pumping of groundwater).....	57

TABLES

Table 2.1: TRT locations in the Oslo region and Kristiansand.....	12
Table 3.1: Overview over the TRT results at borehole 3, Bryn.....	21
Table 3.2: Comparison of thermal conductivity measured <i>via</i> TRTs at the different sites and rock core data.....	24
Table 3.3: Geothermal gradients [°C/km] at the different sites.....	37

1. INTRODUCTION

“Global warming heats up” (Time Magazine, 2009), “The end of cheap oil” (Campbell and Laherrère, 1998), “Greenhouse gases – the highest concentration since 800 000 years” (Welt, 2008) are typical headlines in the media reporting about the environmental and energy problems humans are facing. The Intergovernmental Panel on Climate Change, in their latest report from 2007, shows that recent actions in climate politics will not stop or slow down the global change. Their scientific results show that CO₂-neutral renewable energy sources should be developed further and increasingly replace fossil energy sources.

Low-temperature geothermal energy, also called shallow geothermal energy or ground-source heat applications, are considered one of the key technologies to reduce greenhouse gas emissions (Sims et al., 2007). In continental Norway, there has hitherto only been one high-temperature geothermal project. This was abandoned because of drilling problems. “Rikshospitalet”, the new hospital in Oslo, should get 3 MW heat from 3 to 5 km deep boreholes following the Hot Dry Rock (HDR) concept. So far, deep geothermal projects are not cost-effective on the Scandinavian continent and more research is needed (Enova, 2007). Currently in Scandinavia, shallow geothermal energy systems have a higher commercial potential than conventional high-temperature geothermal systems (Enova, 2007). In addition, high-temperature geothermal energy plants do not use a renewable energy source, as exploited heat is not restored rapidly enough. Ground-source heat, on the other hand, may be considered renewable as energy is restored predominantly through a heat flux from the solar heated surface (Banks, 2008).

The so-called “Stern review”, published in 2006 was the first report focussing on the effect of global warming on the world economy. Among other things, it shows the relative greenhouse gas emissions per sector (Fig. 1.1). Buildings (e.g. space heating and cooling) account for 8 % of the total greenhouse gas emissions, or possibly even 20 % if upstream emissions associated with electricity and heat are included (Stern, 2006).

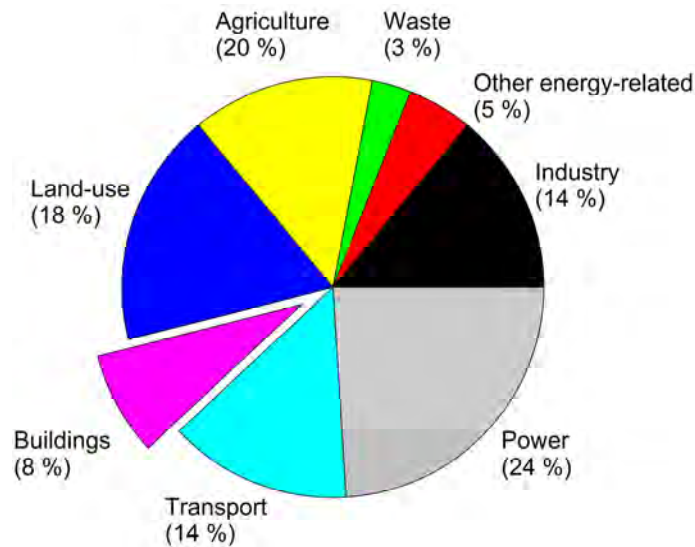


Fig. 1.1: Relative greenhouse gas emissions in the year 2000 by source (Stern, 2006 mod.).

Ground-source heat installations are more environmentally friendly than the use of fossil fuels and electricity only and can help to reduce greenhouse gas emissions in the building sector. There are two different systems of low-temperature geothermal heat installations: a) Open loop systems, if aquifers with high yields are present (in Norway for example in glaciofluvial sediments like at Oslo airport Gardermoen; Midttømme, 2005), or b) closed loop systems where brines circulate through a horizontal or vertical collector pipe in the soil or a borehole (Banks, 2008). The latter technique is widely applied for space heating and if necessary, cooling in summer in northern countries with hard crystalline bedrock. In the case of space cooling, heat can be transferred to the ground in summer which is in turn then available in the following winter for space heating (aquifer and borehole thermal energy storage, ATEs and BTES). Combined systems enhance the energy efficiency. The ground heat is transferred from the collector fluid with the help of a heat pump. In this way temperatures are reached that meet the demands for domestic space heating. In Norway, there were about 15 000 ground-source heat pump installations in operation for heating and air conditioning of single houses and larger buildings in 2005 (Midttømme, 2005), and the number of energy wells reported to the national well database at the Geological survey of Norway (NGU) indicate an annual increase of at least 2 500 installations.

Energy wells for single households as well as those for bigger ground-source heat installations have to be planned and dimensioned carefully to avoid that the necessary energy loads cannot be matched by the ground-source heat pump system. Therefore, it is, among others, important to know the thermal conductivity of the rocks surrounding an energy well

and the well's borehole resistance. Both parameters can be calculated with the help of a thermal response test (TRT) and will be discussed further in the following chapters.

TRTs have been in use in Norway since 1999 and are currently being conducted by the private company Geoenergi AS, the Norwegian Geotechnical Institute (NGI) and NGU.

One aim of this study is to gather all TRT data available for one piloted region, the geologically diverse Oslo field. A large dataset of rock core samples for this region exists at NGU. The method used to determine the rock thermal conductivity is based on Middleton's (1993) approach and is described in detail by Ramstad et al. (2008a). The latter database is visualized in a map over the thermal conductivity of the geological units of the bedrock map for the Oslo region (Lutro and Nordgulen, 2008) which was presented at the 33rd International Geological Congress in Oslo (Ramstad et al. 2008b). This map may become a basis for a suitability map for ground-source heat installations as presented for example in Japan (Fujii et al. 2007).

Two unrelated hypotheses are tested:

I) Effective thermal conductivity values measured via TRTs in the Oslo region (non-grouted, water-filled boreholes) are significantly higher than the lab measured thermal conductivity from rock cores.

II) Thermal conductivity maps (like the one of Ramstad et al. 2008b) based on surface rock core data can replace TRTs.

Another aim of this study is to characterize the influence of groundwater in a fractured aquifer on the effective thermal conductivity measured in an energy well. Groundwater can affect the measured effective thermal conductivity in three ways, 1) through advective heat transport in flow direction, 2) convective heat transport in a non-grouted and water-filled borehole (including the thermosiphon phenomenon) and 3) to a minor extent through conductive heat transport (thermal conductivity of water is low: $0.6 \text{ W m}^{-1}\text{K}^{-1}$). In earlier studies, a typical approach was to use numerical models where groundwater and heat flow were combined. Typically, the advective heat transport with groundwater was simulated for porous media (Fujii et al. 2005; Jiang and Woodbury, 2006; Pannike et al., 2006; Fan et al. 2007; Lee and Lam, 2009) and in few cases also for hard rock (e.g. fractured) aquifers (Chiasson et al. 2000; Gehlin et al., 2003; Gehlin and Hellström, 2003). Also lab experiments focus so far mostly on

porous media (Katsura et al., 2006; Katsura, 2009). *In situ* experiments investigating the influence of groundwater flow on TRTs have rarely been performed in porous aquifers (Witte, 2002).

By contrast, in this study a field experiment in a fractured aquifer was performed with pumping of groundwater to induce an artificially controlled groundwater flow towards a second well. In “Annex 21 TRT” of the International Energy Agency (IEA) it was raised the question how groundwater flow can be detected in a TRT.

Two unrelated hypotheses are tested for this reason in the second sub-project of this study:

I) Groundwater significantly influences the effective thermal conductivity in hard rock aquifers measured with a TRT.

II) Lateral groundwater flow can be detected in temperature profiles after TRTs.

Hypotheses are discussed in the “global evaluation” (Chapter 4).

2. METHODS, EQUIPMENT AND INVESTIGATION SITES

A TRT measures the effective ground thermal conductivity. The value integrates thermal conductivities of rocks with varying mineral contents along the whole borehole. The standard test equipment which has been used in this study was described in detail by Gehlin (1998) and is shown during operation in Fig. 2.1. The TRT trailer is connected to the collector pipes of the energy well. Heating elements heat the brine which is circulating through the closed loop system and the trailer. The connection between the trailer and the borehole has to be insulated properly to avoid heat loss or gain (through sun irradiation). The circulation pump creates a turbulent flow in the pipes to get best heat transport from the collector towards the ground. The undisturbed ground temperature (measured before the TRT) and the temperature increase in the brine during a test run is used to calculate the effective thermal conductivity of the ground λ and the borehole resistance R_b . The latter parameter is a measure for the thermal resistance between the heat carrier fluid in the collector pipes and the borehole wall (depends on the arrangement of the collector pipes and the thermal properties of all materials involved). The calculation of the thermal conductivity and the borehole resistance follows the

suggestions of Gehlin (2002) which is based on the line-source theory (Ingersoll, 1948). A TRT lasts ideally 72 hours.



Fig. 2.1: TRT rig during operation at Sørlandssenteret, Kristiansand.

Sources of errors are: 1) heat leakages, 2) variable electric power supply, 3) accuracy of the determination of the undisturbed ground temperature and 4) free convection of water in non-grouted boreholes (standard for energy wells in Scandinavia), 5) gradient-driven horizontal and 6) density-driven vertical groundwater flow (e.g. thermosiphon effect, Gehlin et al., 2003, Gustafsson, 2006).

Temperature profiles were taken with the help of temperature dataloggers (VEMCO, 8-bit Minilog TDR, Halifax, Nova Scotia, Canada) with a sinker bound to a 200 m long chord (Fig. 2.2).



Fig. 2.2: VEMCO minilogger and sinker bound to a chord with two meter marks for manual depth determination (left) and temperature logging inside the collector pipe (right).

Temperature profiles were then taken inside the collector pipe before each TRT to determine the undisturbed ground temperature and four hours after the end of the TRT. The time interval for a standard temperature profile was set to two minutes to ensure that the datalogger adapts to the fluid temperature even at steep temperature gradients. The depth interval was two meters for the measurements down to a depth of 40 meters. Below and until the end of the borehole the resolution was 4 meters. There, lower temperature variations can be expected. Additionally, it is necessary to keep the measurement of a temperature profile short to avoid a further temperature recovery in the case of the measurement after a TRT. The depth interval was set to four meters. For a 200 m deep borehole the measurement of one temperature profile takes accordingly 70 minutes (30 minutes for the first 40 m and 40 minutes for the next 160 m). This standardized method is necessary to compare the temperature recovery in different wells in different hydro-, thermo- and geological settings. For all temperature profiles performed four hours after the TRT, it has to be kept in mind that there is a temperature recovery during the measurement. A permanent temperature log after a TRT in Bryn (see chapter 2.1) in 30 m depth showed a recovery of 0.5 °C between 4 and 5 hours and 10 minutes after the test.

2.1 BRYN

2.1.1 Site description

The well field of Bryn (32 583649E, 6643494N, ca. 60 m asl) is located 14 km west of the city of Oslo and ca. 30 m west of the river Lomma (see Fig. 2.9, p.12). A centre well and four satellite wells form the well field. The boreholes were drilled in the year 2000 taking into account structural geological pre-investigations of Larsen (2001) so that boreholes 1, 3 and 5 were placed parallel to the strike of the bedding. Boreholes 2 and 4 form a line perpendicular to the strike (Fig. 2.3, detailed discussion of the geology is found below).

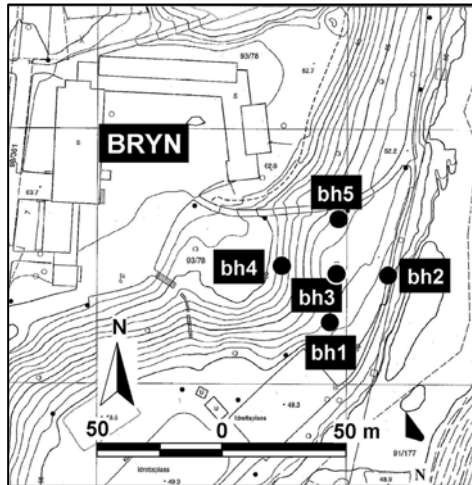


Fig. 2.3: Map of the well field at Bryn, Bærum municipality (Ramstad 2004).

All boreholes are 100 m deep and have a diameter of 5.5'' (140 mm). The well field was originally drilled as a pilot plant for ground-source energy use with an open loop system. Groundwater was planned to be circulated using the centre borehole (bh3) as injection well and the satellite wells (bh1, bh2, bh4, bh5) as production wells. To improve the well yields, hydraulic fracturing with water and sand as propping agent was performed and a test run started in 2003. All boreholes (except bh4) showed significantly improved well yields after fracturing. Only a low circulation rate, however, was achieved due to too low infiltration capacities of borehole 3 (Ramstad et al., 2007).

In the present study, boreholes 3 and 2 are investigated further.

2.1.2 Geology

The geology in Bryn is dominated by a low-grade metamorphic sandstone of the Ringerike group. While the Ringerike sandstone deposits originally were about 1000 m thick, at Bryn they might be still as thick as 350 m (Larsen, 2001). During the late Silurian, river delta and shallow seawater sediments formed with a shoreline advancing towards south with a sediment transport arriving from the Caledonian mountains (Davies et al., 2005). Ripple marks were found in direct vicinity of the well field (Fig. 2.4). The closest outcrop lies about 30 m east of the well field and follows the bed of river Lomma. Due to a low water level in the river during the investigation a broad inspection of fractures was possible. The dominating fracture set is the one parallel to the bedding. It is also the most likely direction to keep fractures open due to vertical pressure release after the melting of the Scandinavian ice sheet after the last Ice

Age (Rohr-Torp, 1994; Morland, 1997). Thirty bedding planes led to mean strike/dip values of $35^\circ \pm 12^\circ / 6^\circ \pm 2^\circ / \text{SE}$. Groundwater flow through these fractures is expected.

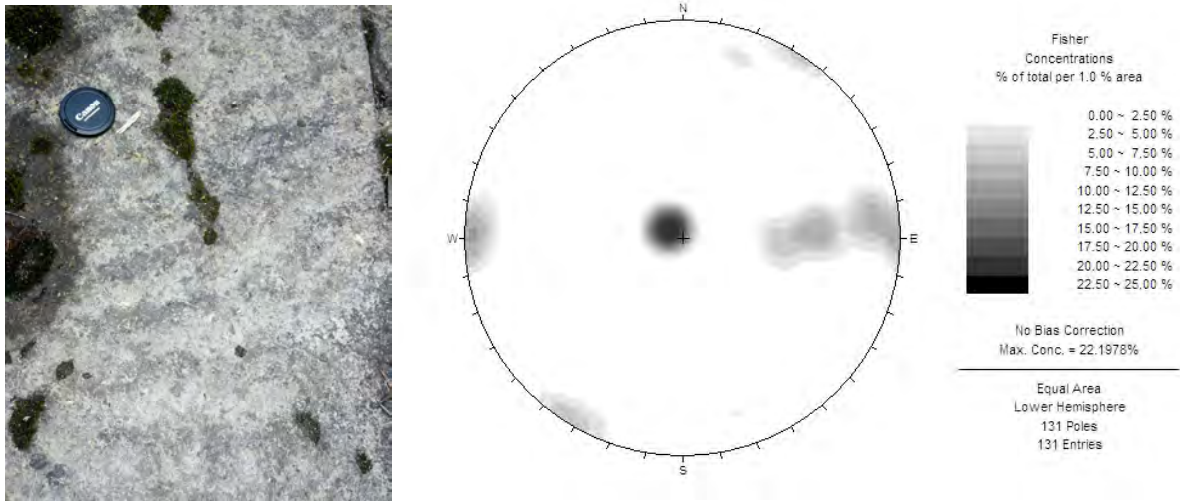


Fig. 2.4: Ripple marks on bedding surface (left) and Fisher fracture stereogram (right) showing the poles to strike and dip data collected along river Lomma at low water level.

Two fracture sets striking approximately N-S can be interpreted as extensional fractures belonging to normal faults that appear in the area ($177^\circ \pm 8^\circ / 56^\circ \pm 18^\circ / \text{WWS}$, n: 45 and $6^\circ \pm 19^\circ / 81^\circ \pm 19^\circ / \text{EES}$, n: 15). They might be open sometimes but observations at the surface indicate rather that they are closed in most cases. Minor fracture sets with fractures which are very likely to be closed show a strike/dip of $102^\circ \pm 22^\circ / 80^\circ \pm 8^\circ / \text{NNE}$ (n: 17) and $107^\circ \pm 14^\circ / 76^\circ \pm 10^\circ / \text{SSW}$ (n: 10) (see also Fig. 2.5).



Fig. 2.5: a) View towards NE along the river valley of Lomma. Notice the large exposed bedding planes and dominant fracture sets striking N-S. b) fractures of all fracture sets besides the one parallel to the bedding are filled with quartz (light grey veins in the bluish sandstone).

The fracture analysis stereogram (Fig. 2.4) showing the fractures at the surface is in accordance to stereograms of the fractures along the different boreholes at Bryn measured earlier with an optical televiewer (Ramstad, 2004).

For borehole 3 (the well which was used for a TRT in this study) the layer with unconsolidated sediments is 1.3 m thick. The first 50 m of the borehole are dominated by sandstone bands (20 to 50 cm thick) alternating with thin layers of clay (1 to 2 cm thick). Below 50 m the rock type turns into a darker sandstone/siltstone. Mafic igneous dykes appear. Open fractures have been reported at 13 m and 90 m depth (Midttømme et al., 2004).

2.1.3 Hydrogeology

Investigations of Larsen (2001) show that the rock consists of quartz rich, well-compressed sandstones of low matrix porosity, so that significant groundwater flow is expected only in open fractures. The study of Ramstad et al. (2007) shows a well yield of around 1900 l hr⁻¹ and 2500 l hr⁻¹ in borehole 2 and borehole 3, respectively, after hydraulic fracturing with the injection of sand. As hydraulic fracturing was performed in the year 2003, the well yield may have declined since then due to possible clogging in fractures and precipitation of iron and manganese compounds. The well yield before hydraulic fracturing was 370 l hr⁻¹ and 320 l hr⁻¹ in borehole 2 and borehole 3, respectively. This indicates that the well yield should lie in between the latter values and the values directly after hydraulic fracturing. The presence of igneous dykes has been reported to increase groundwater flow, not restrict it in the Oslo region (Løset, 1981, 2002; Boge et al., 2002). The reason might be fracturing during fast cooling of intruding rocks.

Groundwater drawdown and recovery test (single-well)

Hydraulic parameters can be measured with the help of aquifer tests. Groundwater was pumped at a rate of 2.2 l s⁻¹ (7.92 m³ h⁻¹) for 115 hours so that steady state conditions were easily reached. When the pump in borehole 2 was switched off, the rise-up of the groundwater table was measured (Fig. 2.6). The pump (Grundfos SP 5A-12, Grundfos Management A/S, Bjerringbro, Denmark) was installed close to the bottom of the well at 85 m depth.

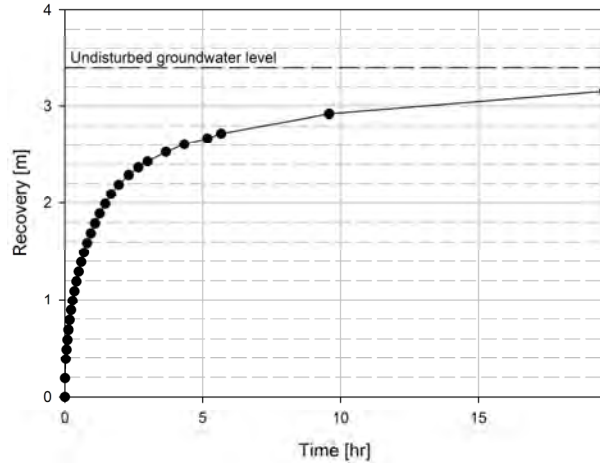


Fig. 2.6: Recovery from steady-state conditions at borehole 2 with previous pumping of groundwater at a production rate of $2.2 \cdot 10^{-3} \text{ m}^3 \text{ s}^{-1}$.

The data were used to calculate an overall value for the hydraulic conductivity, $5 \cdot 10^{-6} \text{ m s}^{-1}$ which is in accordance to the range given for both porous sandstones ($3 \cdot 10^{-10} \text{ m s}^{-1}$ to $6 \cdot 10^{-6} \text{ m s}^{-1}$) and for fractured metamorphic rocks ($8 \cdot 10^{-9} \text{ m s}^{-1}$ to $3 \cdot 10^{-4} \text{ m s}^{-1}$; Domenico & Schwartz, 1998).

The calculated value, however, has to be understood as a rough pseudo-parameter as the flow field is dominated by a main fracture covering the whole borehole field in 12 to 17 meters below the surface. This fracture must be rather wide and open as the groundwater level at all wells of the well field reacts exactly parallel to the changes observed in the production well (Fig. 2.7).

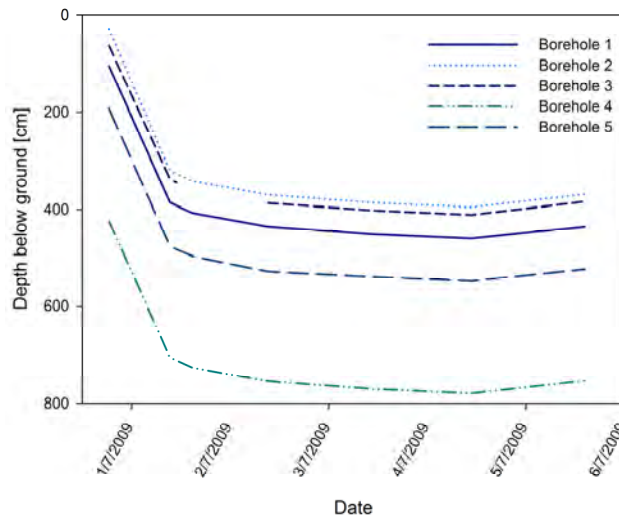


Fig. 2.7: Parallel drawdown of the groundwater level in all boreholes of the well field in Bryn, groundwater level at borehole 3 was not measured on 02.07.2009.

Models adapted to fractured petroleum reservoirs like the ones of Barenblatt et al. (1960) or Warren and Root (1963) are not adaptable to this situation as they divide the reservoir (or

equivalent to it: the aquifer) in a regular arrangement of blocks and fractures which is not the case either.

2.1.4 Thermogeology

A standard U-shape PE collector pipe (40 mm diameter) was installed in borehole 3 and a standard TRT was performed.

In addition, a second TRT was performed with pumping of groundwater from borehole 2 so that an artificial groundwater flow towards this well was induced. The water was transported away from the influence area with the help of a fire hose (Fig. 2.8). Both TRTs were performed with two heating elements à 3 kW. Temperature profiles were taken before and four hours after both TRTs. The temperature profiles before the TRT allow for the calculation of the undisturbed ground temperature. Furthermore, they give indications about the geothermal gradient in the depth and the heat flow along the whole borehole. The temperature profiles after the TRTs are used to interpret variations in temperature recovery of the ground due to groundwater flow or varying thermal properties of different rock layers.



Fig. 2.8: TRT setup at borehole 3 for the test with pumping of groundwater and water removal with a fire hose.

2.2 OSLO REGION

Seven boreholes in the Oslo region and Kristiansand were investigated for their thermal properties (Fig. 2.9, Table 2.1).

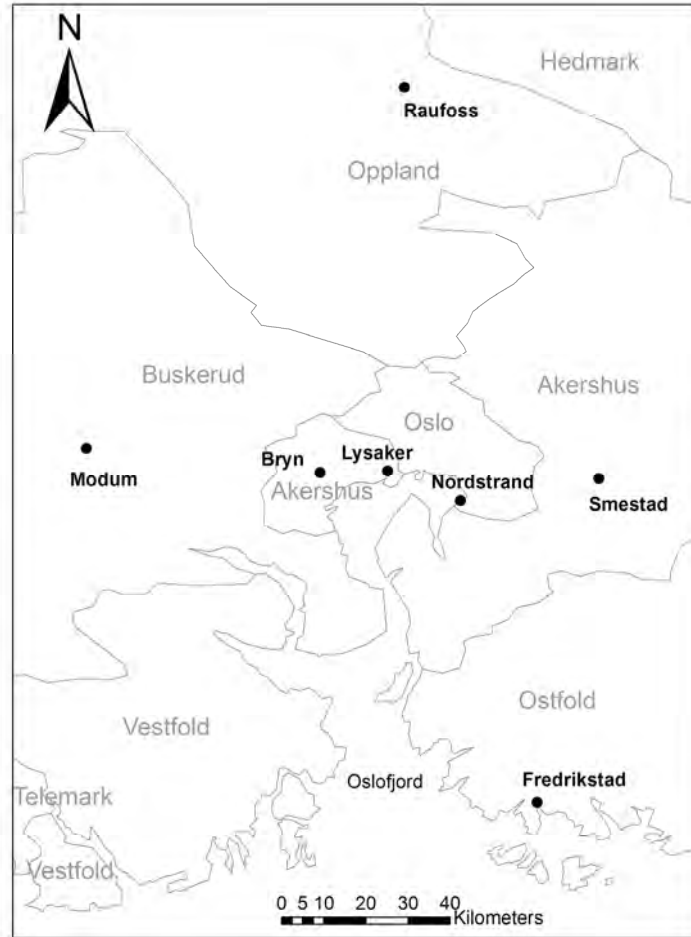


Fig. 2.9: Overview of locations where TRTs were performed in the Oslo region (bold) in different counties.

Table 2.1: Coordinates of TRT locations in the Oslo region and Kristiansand.

Site	Zone	E coordinate	N coordinate	Altitude [m asl]	Borehole depth [m]
Bryn	32	583649	6643494	60	100
Fredrikstad	32	611848	6565630	17	200
Kristiansand	32	448659	6448847	70	200
Lysaker	32	591697	6644080	30	180
Modum	32	555683	6648713	77	200
Nordstrand	32	600555	6637162	130	200
Raufoss	32	591370	6735349	429	200
Smestad	32	616946	6642954	204	200

The boreholes were drilled as test energy wells or for ground-source heat installations and have been made available for thermal response testing before finishing by Båsum Boring AS,

Futurum Energi AS and the Norwegian Geotechnical Institute (NGI). Boreholes were mostly drilled with a diameter of 115 mm. Casings are used where unconsolidated materials overlay the bedrock to prevent slides.

In all boreholes TRTs were performed and temperature profiles measured before and four hours after the TRTs. Additionally, the regional geology was investigated at nearby outcrops to get an indication for fracture areas or variations in the rock type. Well reports were provided by the drilling companies (Båsum Boring AS and Vann & Energi Sør AS) and give further information about all wells.

The surface rock types at the different locations are shown in Fig. 2.10 if outcrops were present close to the investigation wells.

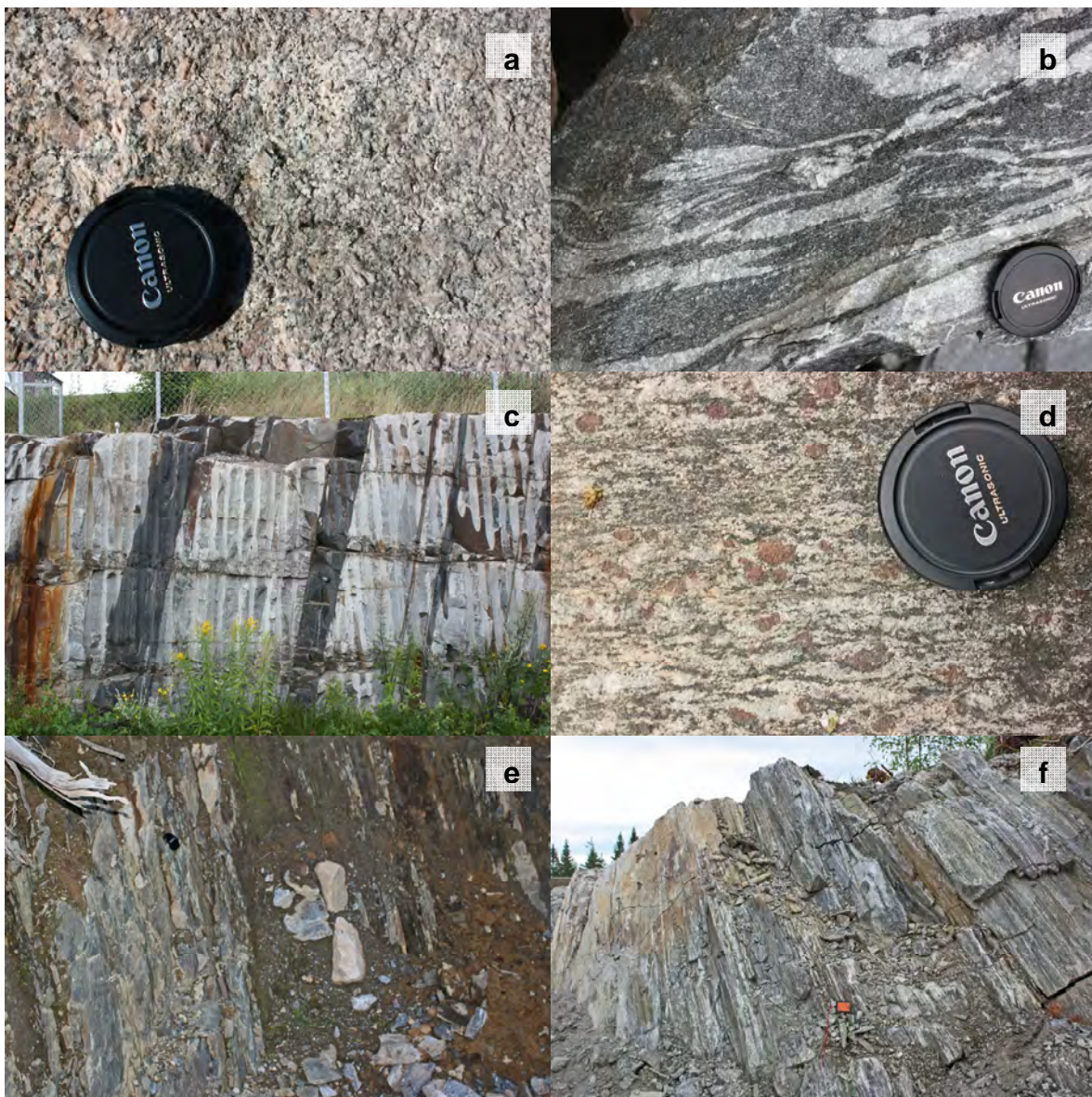


Fig. 2.10: a) Iddefjord granite (Precambrian, Fredrikstad), b) migmatitic gneisses (Precambrian, Kristiansand), c) banded gneis with mafic dykes parallel to the foliation (Precambrian, Modum), d) garnet-rich gneis (Precambrian, Nordstrand), e) limestone (Late Ordovician, Raufoss), f) banded gneis (Precambrian, Smestad), not shown: Ordovician limestone/shales at Lysaker (no outcrop close-by could be found).

Short description of the geology at the different sites:

2.2.1 Fredrikstad

Outcrops close to the boreholes at Fredrikstad consist of rather homogeneous light reddish, biotitic, intermediate grained "Iddefjord granite" which intruded in the Precambrian around 920 – 930 Ma ago (Pedersen and Maaloe, 1990). It contains quartz, biotite, orthoclase, plagioclase, some muscovite, apatite, titanite, magnetite and zircon (Holtedahl, 1953). It is interpreted as the continuation of the "Bohus granite" in Sweden. Regional fracture zones appear but show low hydraulic transmissivity because of the appearance of swelling-clay minerals due to hydrothermal alterations and/or deep weathering in the Triassic and Jurassic period (Banks 1992a,b; 1994; Olesen et al., 2006).

Slagstad et al. (2009) measured a thermal conductivity of $3.1 \text{ W m}^{-1}\text{K}^{-1}$ in the Iddefjord granite.

2.2.2 Kristiansand

All outcrops within the range of 100 meters around a planned well field including the test well were mapped geologically. The dominating rock types are gneisses of different colour and mineral content which may show a wide range of thermal conductivities. As an average thermal conductivity $2.9 \text{ W m}^{-1}\text{K}^{-1}$ is recommended in Earth Energy Designer v. 2.0 (2000) if no *in situ* measurement can be done. The northern outcrops are biotite rich whereas southern outcrops show a higher feldspar and quartz content. In several parts migmatitic structures appear (Fig. 2.10). Folding appears at the site. The folds are so large, however, that no complete folds could be found at the outcrops.

The main fracture direction is parallel to the foliation of the gneisses ($56^\circ / 51^\circ \text{ NW}$, n: 31) and fits the findings of Falkum (1972) who suggests a complex megatectonic Precambrian fold with N-S striking axis about 40 km west of Kristiansand which affects the whole Agder-Rogaland region. There has been obvious tectonic movement along the main fracture planes (sinistral, normal faulting, Fig. 2.11). Fracture surfaces show a brownish cover of iron precipitates that form in presence of groundwater. Cataclastic rocks appear in thin zones between the moved layers (Fig. 2.12). They may act as groundwater flow barriers due to their fine-grained material.



Fig. 2.11: Apparent normal fault forming open fracture planes, orange arrows show a pegmatitic (pink) dyke, among others, used as indicator for the movement direction.



Fig. 2.12: Cataclastic contact between two moved layers.

Fractures at all outcrops were measured. Fig. 2.13 shows that the main fracturing appears parallel to the foliation direction. Other fracture directions are much less pronounced. A second subset of fractures strikes around 135° and dips with 65° towards north-east. The dominating fractures are most likely to show elevated hydraulic conductivities.

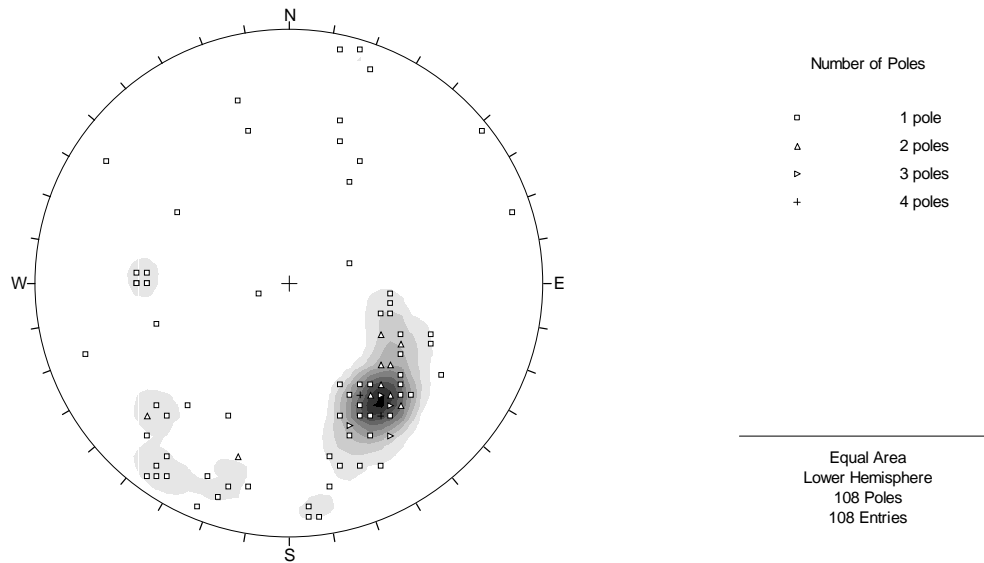


Fig. 2.13: Equal area stereonet (lower hemisphere) showing the poles to open fractures (n:108).

2.2.3 Lysaker

No outcrop was found nearby and all information about bedrock has been taken from the literature. The geological map of Asker (Naterstad et al., 1990) indicates shales with nodular limestones for the site of the investigation well, belonging to the Ordovician sediments of the Oslo Group (Vollen Formation). The nodular limestones are secondarily formed. The dark shales indicate that the sediments were deposited in a badly ventilated oxygen-poor sea. Limestone bands that might appear as well along the borehole were formed during times when a clear and shallow ocean was present. These conditions are necessary for most limestone forming organisms (corals, brachiopods, crinoids...; Holtedahl, 1953).

The thermal conductivity expected for this kind of rock is similar to the one at Raufoss ($2.4 \text{ W m}^{-1}\text{K}^{-1}$).

2.2.4 Modum

The bedrock map of the Oslo region (Lutro and Nordgulen, 2008) indicates different kinds of Precambrian gneisses and amphibolites as well as Permian rhomb-porphry dykes for the area around the study well. The closest outcrop was found 300 m southwest of the well (32, 555436E, 6647984N). It showed banded gneisses with a strike and dip of the foliation of $139^\circ \pm 3^\circ / 76^\circ \pm 3^\circ / \text{SW}$ (n: 4). Mafic diabase dykes were about 20 cm wide and striked parallel to the foliation (see Fig. 2.10). They are related to the Permian volcanic activity in the Oslo

graben. As an average thermal conductivity value, $2.9 \text{ W m}^{-1}\text{K}^{-1}$ is suggested for gneisses and $1.7 \text{ W m}^{-1}\text{K}^{-1}$ for diabase (basalt) in Earth Energy Designer v. 2.0 (2000).

2.2.5 Nordstrand

The area around the investigated well field is dominated by garnet-rich tonalitic gneisses few kilometers west of the Mysen syncline (1660 – 1500 Ma; Graversen, 1984; Lutro and Nordgulen, 2008).

Sheet silicates like biotites are a main component of the gneisses at Nordstrand. They are responsible for a strong anisotropy effect in their thermal conductivity. Clauser and Huenges (1995) investigated the thermal conductivity of biotites and measured $3.1 \text{ W m}^{-1}\text{K}^{-1}$ parallel to the sheets and $0.5 \text{ W m}^{-1}\text{K}^{-1}$ perpendicular to the sheets.

At an outcrop approximately 50 meters west of the well field, another local rock type was discovered: A felsic pegmatite dyke (Fig. 2.14).



Fig. 2.14: Felsic pegmatite dyke with large feldspar phenocrysts, arrow indicates the boundary with the garnet gneiss.

It is about two meters wide and shows large feldspar and quartz phenocrysts (ca. 10 cm in diameter). Their appearance has been explained with an intruding melt through fractures, followed by slow crystallisation processes from water-rich solutions (Dons et al., 1996).

The thermal conductivity of the gneiss should be somewhat lower than that of the pegmatite (2.9 and $3.4 \text{ W m}^{-1}\text{K}^{-1}$, respectively, Earth Energy Designer v. 2.0, 2000).

2.2.6 Raufoss

There was only one small outcrop (2 x 2 m) close to the well showing limestones belonging to the Middle Ordovician sediments of the Oslo region. The stratigraphy of the so-called "Mjøsa Limestone" is described in detail in Opalinski and Harland (1981). The Mjøsa Limestones are approximately 100 m thick and overlay quartz-rich siltstones (Furuberg Formation). The upper boundary is formed by an unconformable contact to coarse quartz sandstones (Helgøya Quartzite; Skjeseth, 1963) which fill up an ancient paleokarst landscape. Close to the well, two rock types were detected. In opposition to the bedded and turned limestones shown in Fig. 2.10, a massive dark reddish siltstone was found in direct contact to the latter rock type. It comprises a high amount of fossile bioturbation features (dominantly straight burrows, Fig. 2.15). The burrows are filled with sand and are cemented with limestone (HCl test). The siltstone itself does not react with HCl.



Fig. 2.15: Dark red siltstone with coarse bioturbation burrows.

During formation these layers were located in a warm shallow ocean (burrows show typical perpendicular orientation to the bedding). Bioclastic limestones and fossile coral reefs are widely found. The area is known to show karst properties which involve dissolution fractures and underground channels.

The thermal conductivities of calcareous siltstone and limestone are expected to be in a similar range around $2.4 \text{ W m}^{-1}\text{K}^{-1}$ (Earth Energy Designer v. 2.0, 2000).

2.2.7 Smestad

At Smestad a large outcrop only 5 meters away from the well allowed a more detailed study of the bedrocks. The Precambrian mica gneisses (ca. 1590 – 1490 Ma old) obviously were heated up strongly during regional metamorphism ($> 600 \text{ }^\circ\text{C}$), so that migmatitic structures

evolved in some parts. The dominant rock type is a banded gneiss with an overall foliation direction of $130^\circ / 64^\circ / \text{SW}$ (see Fig. 2.10 and Fig. 2.16) corresponding to the regional trend in the area (Lutro and Nordgulen, 2008). The gneisses belong to the "Stora Le-Marstrand Group" and are paragneisses (Ramberg et al., 2006). The strong foliation in the banded gneisses will lead to a pronounced thermal anisotropy caused by the thermal properties of the micas as described for the gneisses at Nordstrand (see above).



Fig. 2.16: Banded gneisses (left) and migmatitic gneisses (right) at the same outcrop.

Tectonic activity and the appearance of faults parallel to the foliation direction of the gneisses enhances the probability of the evolution of fractures. In general, however, few open fractures are expected due to the ductile character of the micas. A detailed description of the structural geology of the region is found in Graversen (1984).

The thermal conductivity of the gneisses should vary around $2.9 \text{ W m}^{-1}\text{K}^{-1}$ (Earth Energy Designer v.2.0, 2000).

3. RESULTS AND DISCUSSION

3.1 BRYN

3.1.1 Thermogeology

Both TRTs were performed without major problems. The TRT with pumping of groundwater was done in an extraordinarily hot period with day temperatures close to 30°C . The test equipment had never been used in these conditions before and it was not known that the

power supply decreases inverse proportionally with the reference temperature below the lid of the TRT trailer if the temperature rises above a threshold value of approximately 33 °C (Fig. 3.1).

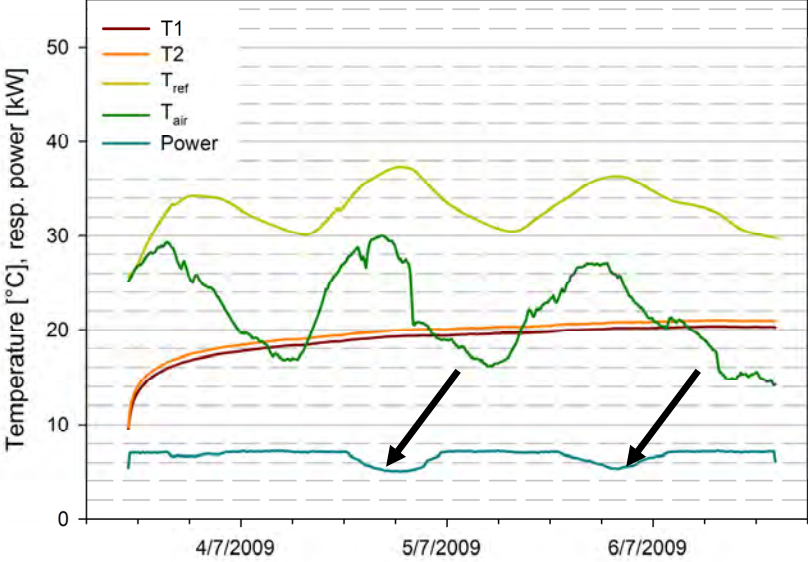


Fig. 3.1: TRT with pumping of groundwater from borehole 2. T1: up-flow temperature, T2: down-flow temperature, T_{ref}: reference temperature inside the TRT trailer, T_{air}: ambient air temperature, Power consumption of the heat elements and the circulation pump. Arrows indicate the decrease in power supply.

The latter problem did not appear during the TRT without pumping of groundwater as the weather was colder and the threshold value was not reached inside the TRT trailer (Fig. 3.2).

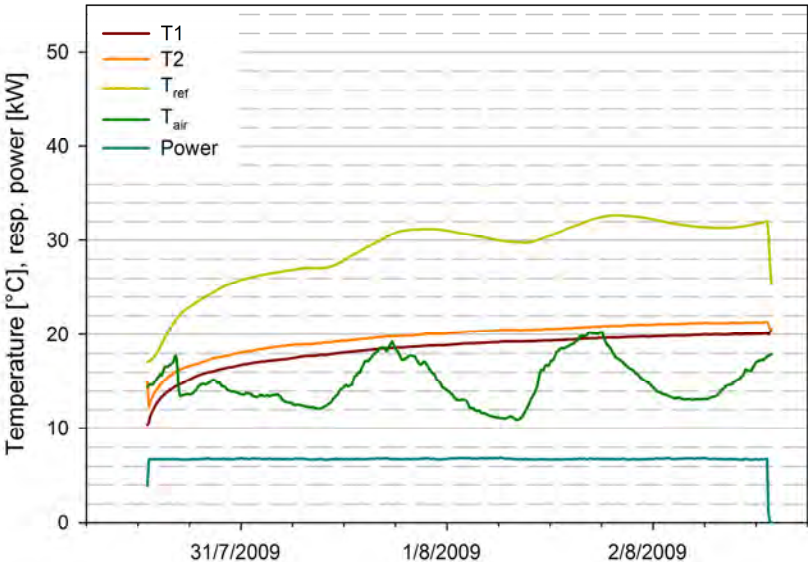


Fig. 3.2: TRT without pumping of groundwater.

The two TRTs were carried out consecutively with a waiting period of 24 days in between. Borehole 3 was heated up during the first TRT to about 21 °C and could recover to about the

same temperature level as before the first TRT. During the waiting time undisturbed groundwater flow conditions in the study area could be reinstalled.

Table 3.1: Overview over the TRT results at borehole 3. The test with alcohol as heat carrier fluid is described in Ramstad (2004).

Pumping of groundwater	Collector fluid	λ [$\text{W m}^{-1} \text{K}^{-1}$]	R_b [$\text{K W}^{-1} \text{m}^{-1}$]
no	alcohol	3.2	0.06
no	water	3.2	0.06
yes	water	3.6	0.06

Table 3.1 gives an overview over the calculated effective thermal conductivities and the borehole resistances for the three tests that have been performed at borehole 3 in Bryn so far. The heat carrier fluid used in the TRT performed by Ramstad (2004) was alcohol to achieve exactly the same conditions as in an ordinary ground-source heat installation. In this study, however, water was used as only negligible different thermal behaviour was expected. Additionally, water has the advantage that any risk of groundwater contamination can be avoided at the site. For all three TRTs the same borehole resistance was calculated (see also APPENDIX B).

In fact, the effective thermal conductivity value of $3.2 \text{ W m}^{-1} \text{K}^{-1}$ could be reproduced in this study. The effective thermal conductivity measured during a TRT with pumping of groundwater led to a value $0.4 \text{ W m}^{-1} \text{K}^{-1}$ higher than without artificially induced groundwater flow. This can be explained by the advective transport of heat away from the well during the TRT with the flowing groundwater. Witte (2002) reports of a similar experiment performed in a porous aquifer in the Netherlands. There, the estimate for the ground thermal conductivity did not converge but increased with time. This effect could not clearly be detected in this study. Possibly the effect is explained by the uneven power supply during the experiment. Assuming that the latter effect is neglectable, maybe the influence of the groundwater flow, limited to a few fracture zones, is of minor importance for the shape of the late brine temperature curve.

The thermal conductivity measured from surface rock core samples led to a median thermal conductivity of $3.46 \text{ W m}^{-1} \text{K}^{-1}$ ($n=24$; Ramstad et al., 2008b). Usually, the effective thermal conductivity measured *via* TRTs gives higher values than lab-measured thermal conductivities. The geology in borehole 3 might be the reason for this exception and it can be

explained with the help of the temperature profile four hours after the TRT (see Chapter 3.1.2).

The borehole resistance was identical in all three tests regardless of the type of collector fluid or whether groundwater flow was induced ($0.06 \text{ K W}^{-1} \text{ m}^{-1}$).

3.1.2 Temperature profiles

In advance of the TRT with pumping of groundwater (TRT1) two temperature profiles were measured in borehole 3, one profile without pumping and one after 14 hours of pumping of groundwater (2.2 l s^{-1}) from borehole 2. No significant temperature difference could be found as the groundwater flowing through borehole 3 and towards borehole 2 might have the same temperature. The mean undisturbed ground temperature before TRT1 was $7.45 \text{ }^\circ\text{C}$. Before TRT2 (TRT without pumping of groundwater) the undisturbed ground temperature was slightly higher ($7.61 \text{ }^\circ\text{C}$) because the waiting time of 24 days was too short to get back to exact undisturbed temperature conditions (Fig. 3.3).

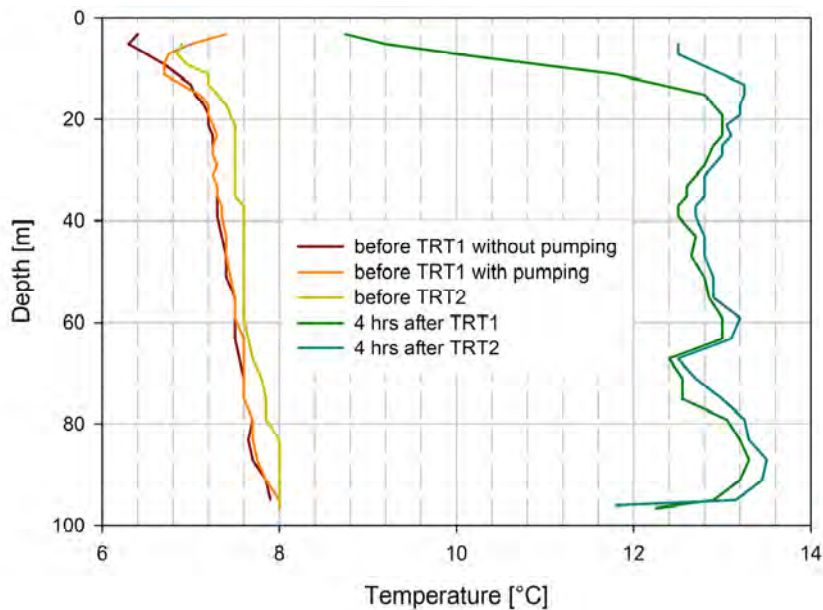


Fig. 3.3: Temperature profiles before and after both TRTs with and without pumping of groundwater.

The temperature profile after TRT2 (without pumping of groundwater) shows one pronounced concavity between 63 m and 77 m with a faster temperature recovery than elsewhere. This might be explained with an enhanced quartz content. Nordstrand (2001) reports a quartz content of 30 % at 63 m depth and 18 % and 26 % at 18 m and 99 m depth, respectively. In this investigation only three samples were taken and analysed with XRD. A diabase dyke

between 17 m and 27 m depth (Ramstad, 2004) was expected to have a lower thermal conductivity than the Ringerike sandstone and in fact, the temperature recovery is rather low in this depth. This explains the lower effective thermal conductivity than the lab-measured value. A clear border with the sandstone, however, cannot be detected in the temperature profile.

To facilitate the comparison between the two temperature profiles after the TRTs, the difference between the mean “undisturbed” ground temperatures ($0.16\text{ }^{\circ}\text{C}$) was subtracted from the temperature profile after TRT2 (Fig. 3.4).

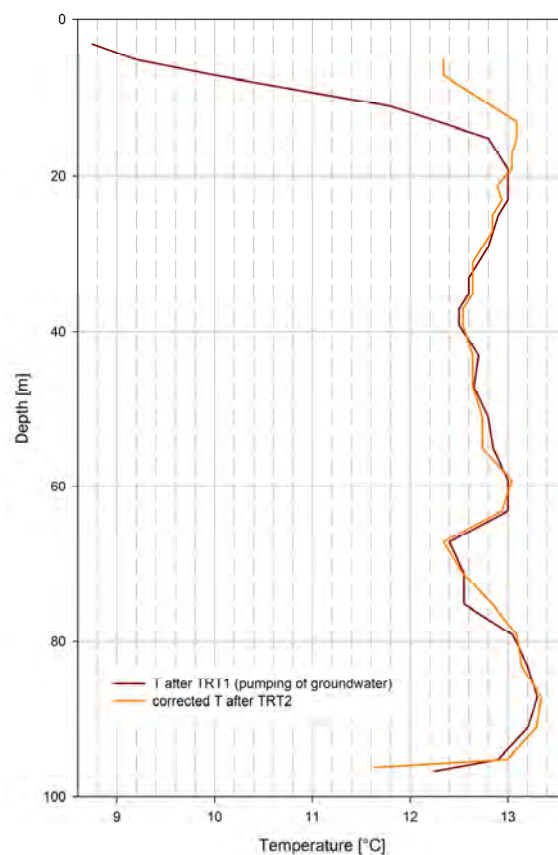


Fig. 3.4: Temperature profiles after TRT1 and TRT2 corrected for the elevated “undisturbed” ground temperature before TRT2.

The temperature curve after TRT1 shows a major deviation from the curve after TRT2 in the first 20 m and a minor deviation at 75 m depth. As the temperature curves cover each other at other depths, these deviations can be explained with a faster temperature recovery due to groundwater flow. A combined flow and heat transport model might give a better understanding for flow velocities and hydraulic conductivities in these zones.

3.2 OSLO REGION

3.2.1 Thermogeology

All TRTs were performed successfully even if electricity outages appeared during the tests in Raufoss and Kristiansand due to cuts in the electricity supply in the whole region. The TRT data from all tests in the Oslo region are shown in APPENDIX A.

The measured effective thermal conductivities were compared with lab measured thermal conductivities from surface rock cores collected throughout the Oslo region (Ramstad et al., 2008b). The rock core data was published in a thermal conductivity map over the Oslo region and is shown in Fig. 3.5.

The measured effective thermal conductivities vary from 2.70 to 3.62 $\text{W m}^{-1} \text{K}^{-1}$ (Table 3.2).

Table 3.2: Effective thermal conductivity measured *via* TRTs at the different sites, median values for the thermal conductivity from surface rock core data belonging to the same geological unit (based on the geological map 1:250 000 of Oslo, Lutro and Nordgulen, 2004) and thermal conductivity of the closest surface rock core to the investigation site.

Site	λ_{eff} [$\text{W m}^{-1} \text{K}^{-1}$]	λ_{Median} [$\text{W m}^{-1} \text{K}^{-1}$]	λ [$\text{W m}^{-1} \text{K}^{-1}$]	Distance [km]	Rock type
Kristiansand	3.20	no data	no data	no data	gneiss
Nordstrand	3.23	3.04 (n=91)	3.33	4.1	gneiss
Smestad	3.62	3.04 (n=91)	3.33	3.7	gneiss
Modum	2.68	4.68 (n=3)	3.31	8	gneiss
Fredrikstad	3.15	3.16 (n=38)	2.50	2.5	granite
Lysaker	2.70	2.70 (n=79)	3.00	1.1	limestone/shale
Raufoss	3.23	2.70 (n=79)	2.17	26	limestone/shale
Bryn	3.20	3.46 (n=24)	2.40	0.4	sandstone

Fractures and fissures are often filled with water but they get (partly) drained in the lab. As air has a lower thermal conductivity than water, *in situ* measurements should lead to slightly higher thermal conductivity values (Ericsson, 1985).

Thermal conductivity of geological units on map sheet Oslofeltet

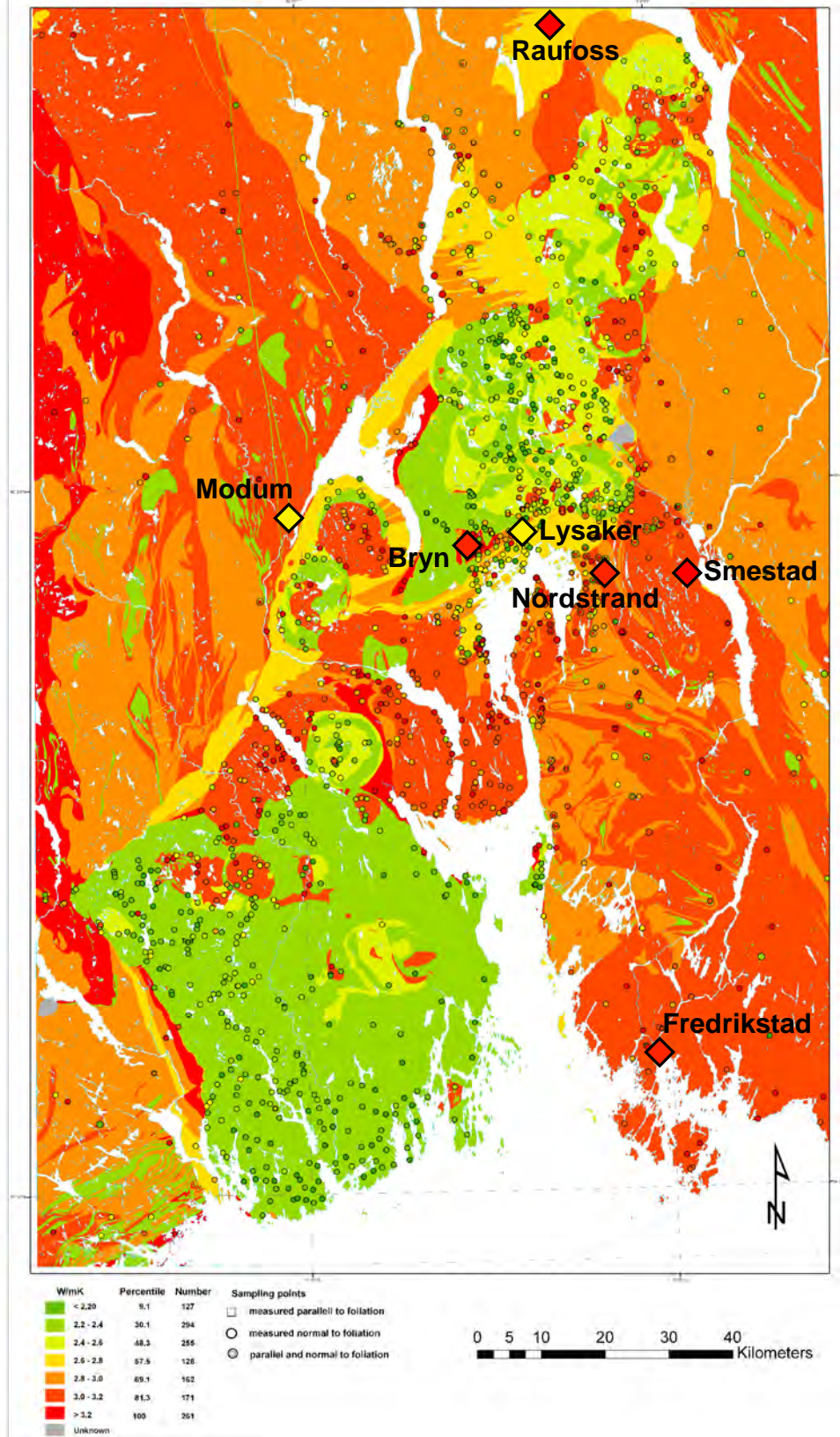


Fig. 3.5: Thermal conductivity map of the Oslo region based on median values per geological unit calculated from lab measurements of surface rock cores (Ramstad et al., 2008b). Rhombs show effective thermal conductivities measured in this study.

Taking into account data of the present study only, the comparison of the TRT results with the thermal conductivity measurement from the closest rock core sample shows no trend (four values are higher and three values lower than lab measured core data of the closest locations, see also Table 3.2).

When the dataset is expanded with available data from TRTs performed since 1999 in the Oslo region, however, in most cases higher effective thermal conductivities have been detected than the rock core sample data would have suggested (Fig. 3.6).

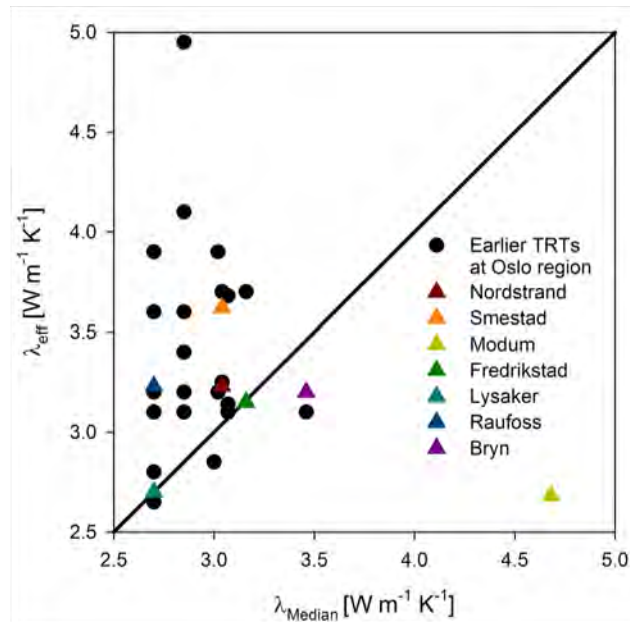


Fig. 3.6: Median thermal conductivity (λ_{Median}) of the according geological unit (Ramstad et al., 2008b) *versus* effective thermal conductivity (λ_{eff}) measured at the different investigation sites of this study (n=7) and of TRTs performed earlier by Geoenergi, NGI, NGU and NTNU (n=34).

The comparison of the effective thermal conductivity at the investigation sites of this study with median thermal conductivities calculated from all core samples belonging to one geological unit show that the results do not correlate. Reasons for lack of correlation may be varying rock types along the well with higher or lower thermal conductivities in comparison to the rocks exposed at an outcrop. Furthermore, natural groundwater flow through the well or in the vicinity of the well (Gehlin and Hellström, 2003) and vertical movement of water (convection and thermosiphon effects, Gehlin et al. 2003) alter the TRT results. The rock core samples may show local variations in their thermal conductivity within the same geological unit and may not represent the rocks actually present at the energy well. The strongly deviating outlier of Modum can be explained with a particularly weak data background for this geological unit with only three scattered rock core samples from a large geological unit.

The data has been classified in igneous, metamorphic and sedimentary rocks and analyzed statistically (Fig. 3.7).

The comparison of the effective thermal conductivities of the three rock classes does not show significant differences (Shapiro-Wilk test for normality and Kruskal-Wallis nonparametric test). One cause might be that the three classes have rather similar average mineral content. Considering a quartz-rich sandstone as an example: It might be metamorphosed and transformed into a paragneiss. Also molten as magma and recrystallized as granite the quartz content can still be similar.

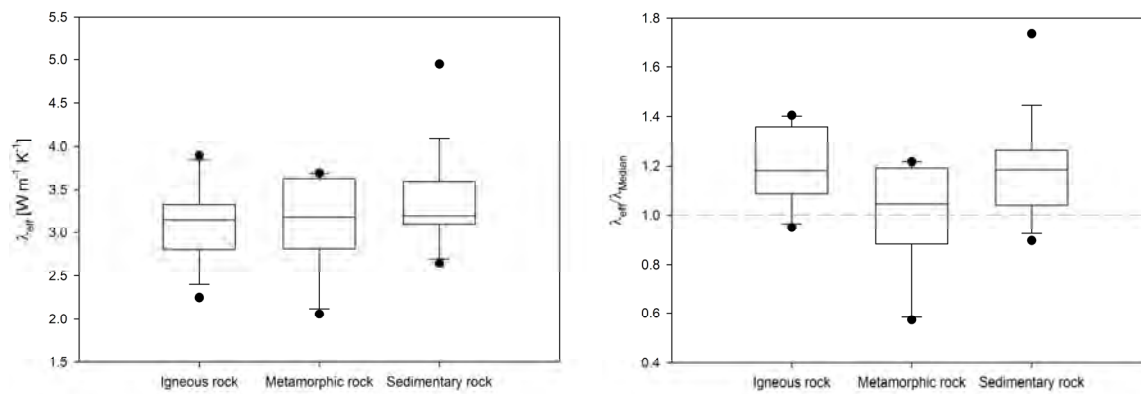


Fig. 3.7: Box and whisker plots for the effective thermal conductivity (left) and the ratio between the effective thermal conductivity and the median thermal conductivity (rock core samples) for igneous (n: 12), metamorphic (n: 10) and sedimentary rock (n: 19) (right).

Dividing the effective thermal conductivity by the median thermal conductivity value obtained from core samples of the geological unit where the respective TRT has been performed, values of 1.0 should be obtained. If the same conditions are met both in the lab and the field measurement all ratios of the different rock groups are higher than 1.0.

Igneous and sedimentary rocks behave in a similar way and no significant difference between the two classes could be found. The metamorphic rocks, however, differ significantly ($P < 0.05$) both from igneous and sedimentary rocks in their thermal conductivity ratio (normality of the dataset and homogeneity of variances allowed for a one-way ANOVA with a Tukey post-hoc test). The variance within the three classes is similar but the average ratio of the metamorphic rocks (1.04) is lower than the one of igneous (1.18) and sedimentary rocks (1.19) and closest to one. Consequently, the mean ratio of the metamorphic rocks indicates that the effective thermal conductivity is approximately the same as the thermal conductivity from the rock core samples (about 4 % higher). The reason might be that the dominant metamorphic rocks in the Oslo region are gneisses containing micas that hinder the evolution

of open fractures due to their ductile character during rock stress. The standard deviation however is high with $\pm 21\%$.

For igneous and sedimentary rocks the effective thermal conductivity is $18 \pm 15\%$ and $19 \pm 20\%$ higher than the thermal conductivity measured from lab samples, respectively. This trend may be explained by the presence of and flow of groundwater.

Even if the dataset for effective thermal conductivity values in the Oslo region is limited (41 samples *versus* 1843 rock core samples), statistical comparisons are possible for some rock types where the sample number is equal to or higher than five. Box and whisker plots are used as descriptive statistics to compare visually the results from the rock core samples with the thermal conductivity data from TRTs. Sufficient data is available for four different geological units (geomap number 7: biotite-rich syenite, geomap No. 25: early Silurian sediments, geomap No. 26: middle and late Ordovician sediments and geomap No. 44: micaceous gneiss, see Fig. 3.8).

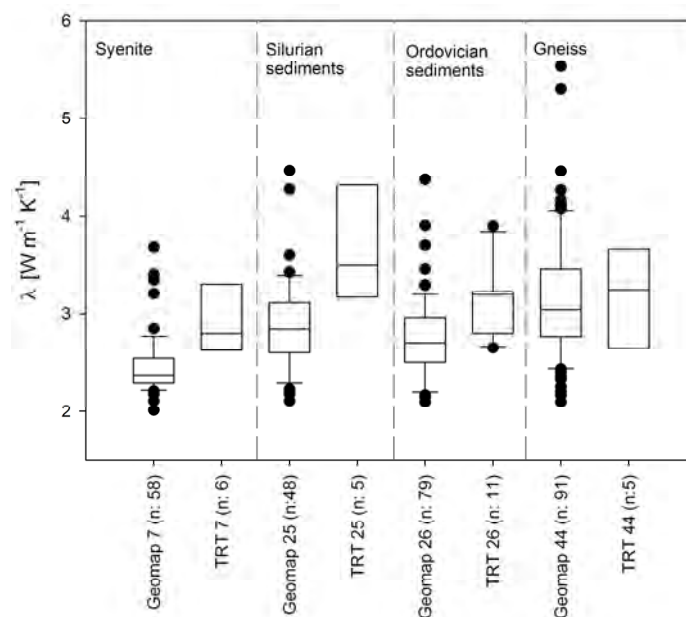


Fig. 3.8: Statistical variations of the thermal conductivity (25 % percentile, median, 75 % percentile, whiskers indicate 10 % and 90 % percentiles if more than 9 samples are available, outliers are dotted) for four geological units of the Oslo region according to the geomap of Lutro and Nordgulen (2004) for data from rock core samples and from TRT data.

Nonparametric Mann-Whitney-U tests show that the thermal conductivities of the rock core samples are significantly different from the values measured *via* TRT in syenite ($P < 0.05$), Silurian ($P < 0.01$) and Ordovician sediments ($P < 0.001$). Instead, no significant difference could be found in the data for the gneiss. Despite the limited dataset a cautious interpretation might be done. Both Silurian and Ordovician sediments in the Oslo region often contain

limestones that may show karst phenomena with a higher probability of groundwater flow. This may explain the significantly higher thermal conductivities from TRTs in comparison to the values from rock cores from Silurian and Ordovician sediments (23 % and 19 % higher median values, respectively). Additionally, the heterogeneity in rock types along boreholes in the sediments may vary more than in thick gneisses and syenites. This might lead to a higher variation in measured effective thermal conductivities. To test this hypothesis the dataset has to be increased. The syenites might be rather homogeneous igneous intrusive rock bodies that were formed during the Permian igneous activity in the region (Rohr-Torp, 1973). The rocks however, were subject to fracturing because of relief of strain. Fractures may be the reason for higher thermal conductivity values due to presence and movement of groundwater, to forced convection and thermosiphon effects or to combined advective water and heat transport. Morland (1997) found a normalised median yield of 22.4 l hr⁻¹ per drilled meter in syenites which is one of the highest yields of the different rock types of this study. The median of the effective thermal conductivity measured in syenites is 18 % higher than the thermal conductivity from the rock core samples which may be explained with groundwater flow through fracture networks.

The micaceous gneisses may have rather few open fractures as biotites (dominating mica) are flexible and do not fracture easily in case of stress. This might explain the finding of no significant difference between the lab measured and *in situ* thermal conductivity. For this example the statistical data basis is poor as 91 rock core samples oppose a small sample number of 5 TRTs in this rock type. An investigation (Morland, 1997) of 3378 boreholes in Precambrian gneisses all over Norway showed that the median normalised yield (16.7 l hr⁻¹ per drilled meter) is much lower than in syenites. A median normalised yield of 11.4 l hr⁻¹ per drilled meter in Cambro-Silurian meta-sediments of the Caledonian mountain chain and the Oslo region is a surprisingly low value which does not prove the hypothesis that there is more groundwater flow in the Ordovician and Silurian sediments. One problem of the results of Morland (1997) is however, that this group contains both stronger metamorphosed sedimentary rocks from the mountain chain that are expected to have lower yields than the weakly metamorphosed sedimentary rocks of the Oslo region.

Kruskal-Wallis tests were used to investigate if there are differences between the rock core samples and TRT samples within the four different rock types (syenites, Silurian and Ordovician sediments, gneisses). No statistical difference is present in the dataset of the TRTs of the four rock types. The reason for that might be the limited number of samples in each subset.

The data indicates that thermal conductivity maps based on rock core samples show low reliability for some geological units. While the thermal conductivity values of metamorphic rocks are close to the values measured in the field, they are more different in the case of igneous and sedimentary rocks. The high standard deviation in all three rock classes does not permit the formulation of general rules.

Statistical analyses were performed with SPSS 17.0 (SPSS, Chicago, IL, USA), box and whisker plots were calculated and drawn with SigmaPlot 11.0 (Systat Software, Chicago, IL, USA).

3.2.2 Temperature profiles

a) Undisturbed temperature profiles

The temperature profiles before the TRTs are not only important to calculate the average undisturbed ground temperature, but additionally they give an indication about the (geo-) thermal gradient and heat flow in the area below a certain depth.

The temperature profile of Fredrikstad was chosen to show how thermal gradients and heat flow data were calculated following Fourier's law:

$$Q_{heat} = -\lambda \frac{d\theta}{dx}$$

where	Q_{heat}	heat flow [W]
	λ	thermal conductivity [$\text{W m}^{-1}\text{K}^{-1}$]
	$d\theta/dx$	thermal gradient [W m^{-1}]

20 m intervals from the temperature profile were used to calculate a thermal gradient value. If a temperature profile starts at 10 m depth, the first thermal gradient value is calculated by the difference between the temperatures at 30 m and 10 m depth. This value is assigned to the depth of 20 m. The same procedure is done for every single step in depth.

Using the thermal conductivity value achieved *via* the TRT performed in the same borehole ($\lambda = 3.2 \text{ W m}^{-1} \text{ K}^{-1}$) and the measured thermal gradient for a certain depth interval, the heat flow is calculated (see Fig. 3.9).

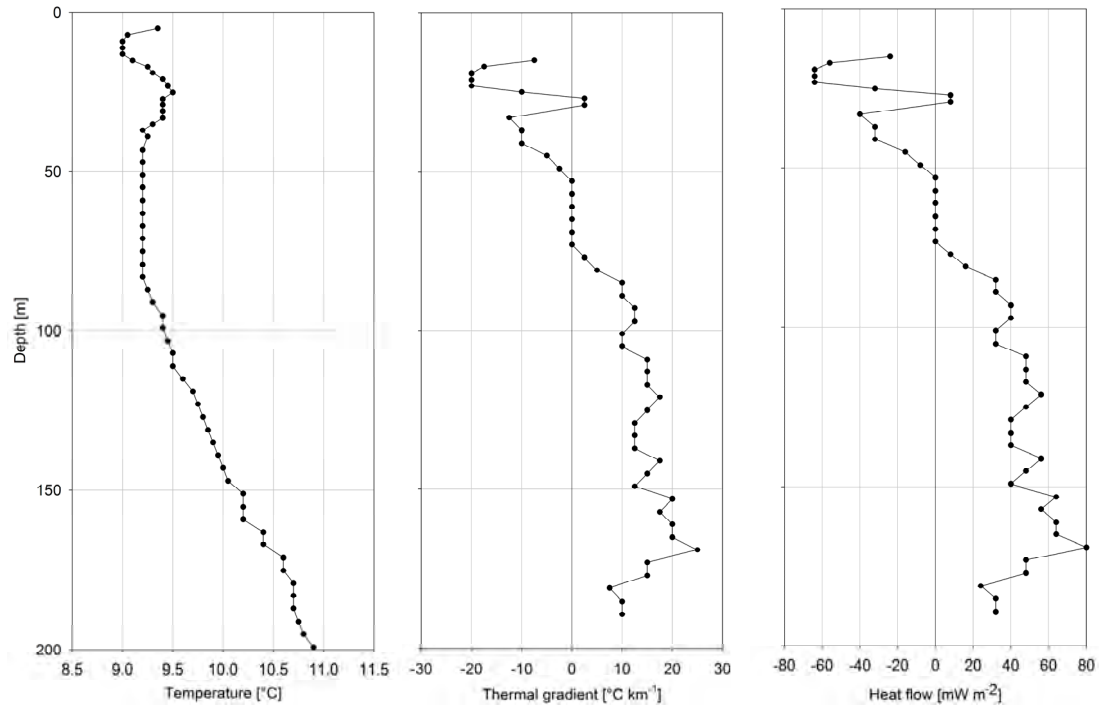


Fig. 3.9: Temperature profile, thermal gradients and heat flow data for the whole borehole depth of 200 m at Fredrikstad. 20 m intervals have been used to calculate the thermal gradient and heat flow data.

Geothermal heat flow varies widely throughout Norway and Fennoscandia. Average heat flow values for different geological provinces of Fennoscandia vary from 34 to 82 mW m⁻² (Slagstad et al., 2009). The mean geothermal gradient for this dataset is 14.6 ± 4.0 °C km⁻¹ and the mean heat flow is 46.7 ± 12.8 mW m⁻² if only data below 80 m depth are taken into account (see Fig. 3.10). Heat production contained in the data should be around $6.3 \mu\text{W m}^{-3}$ (Slagstad et al., 2009).

As heat extracted from the ground is restored both through the heat flux from the surface (atmospheric heat flux plus irradiation) and to a minor degree from the ground (heat dominantly from radioactive decay and residual heat from planetary accretion, Turcotte and Schubert, 2002), a high geothermal gradient and heat flux is still positive for the heat extraction of a low temperature geothermal installation. The geothermal gradient and heat flow are easy to calculate and thus represents inexpensive extra data available through the standard temperature profile before a TRT.

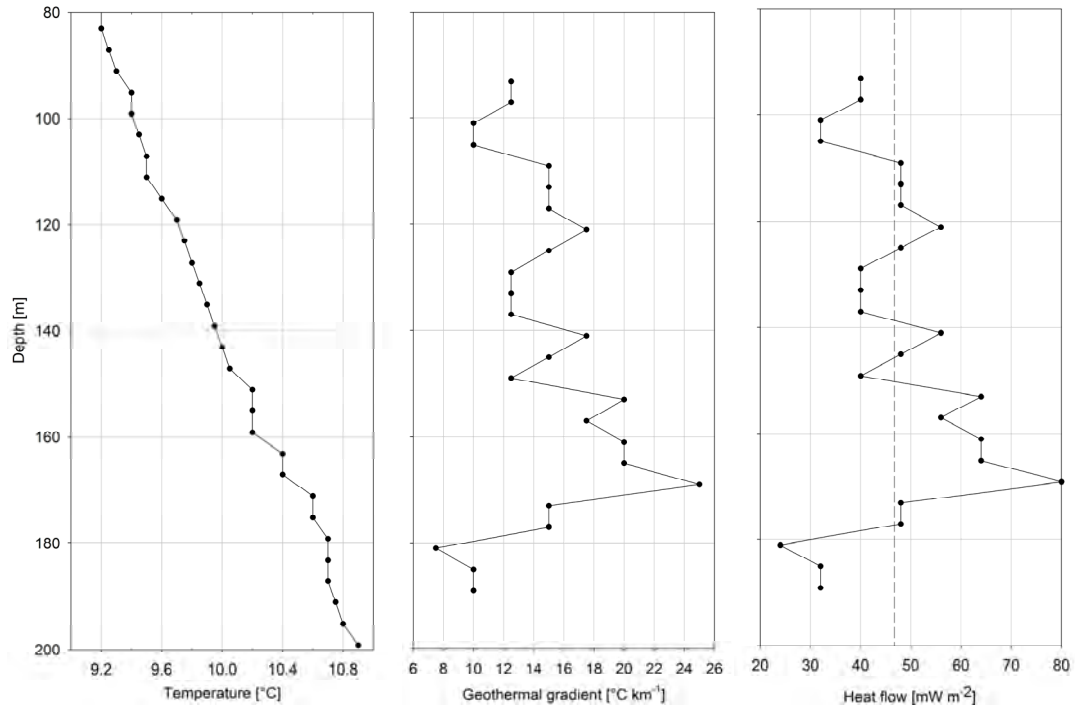


Fig. 3.10: Temperature profile, geothermal gradient and heat flow for the depth of 80 – 200 m below surface level at Fredrikstad. 20 m intervals have been used to calculate the geothermal gradient and heat flow data. Dashed lines indicate the arithmetic mean.

b) Temperature profiles after TRTs

All temperature profiles measured in this investigation were used to calculate heat fluxes (see Fig. 3.11). A trend towards a heat flux typical for a geothermal gradient can be detected below approximately 100 m. Above a certain threshold value there are several variables altering the heat flow, such as change in the average air temperature at the site (local warming for example) or a change in the structure of the surface (shade/sun, slope and exposition, albedo). Below this threshold value it has to be kept in mind that the measured heat flow values might be affected by the paleoclimatic conditions at the site down to at least 1000 m depth (Kukkonen et al., 1998). The last glaciation in the Oslo region should have covered the whole area, so that no pronounced local differences caused by the paleoclimate are expected. Groundwater flow can produce anomalous underground temperatures similar to those expected from climatic change (Lewis and Wang, 1992).

The different wells show no parallel behaviour. Remarkably high heat flow from the surface towards the ground can be observed at Kristiansand and Nordstrand. Both wells are influenced by "thermal pollution" from buildings (see also sub-chapter e). Following the same approach to calculate the heat flow as for the temperature profiles in advance of a TRT, the heat flow calculated from temperature profiles after TRTs show different characteristics.

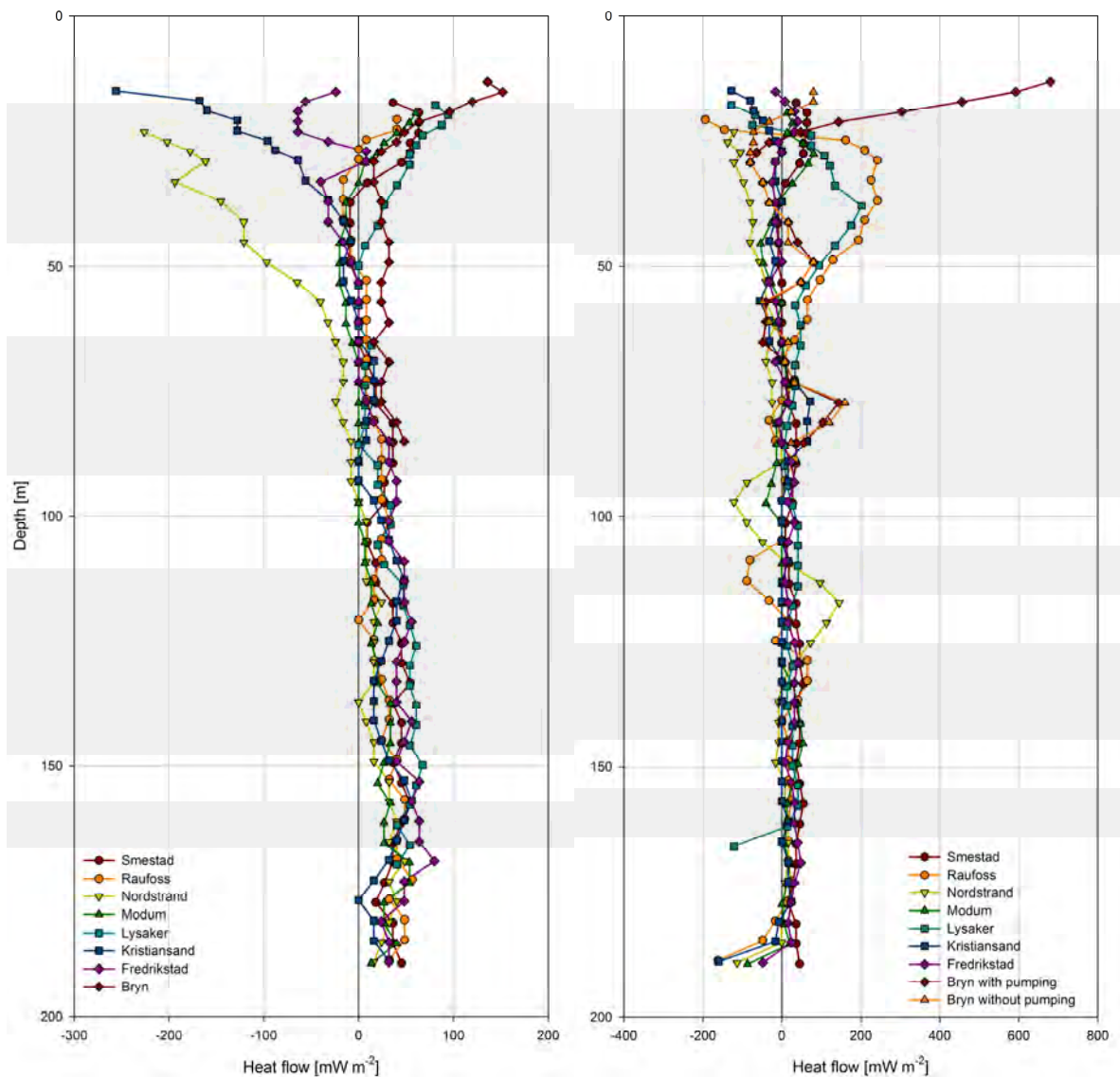


Fig. 3.11: Heat flow calculated for 20 m depth intervals at the different sites calculated from temperature profiles before (left) and four hours after TRTs (right).

In general, the variation in the heat flux data from the different wells is less pronounced. Strong deviations can be seen especially for the heat flow profiles from Raufoss, Nordstrand, Lysaker and Bryn (with pumping of groundwater). They have in common that larger "positive" heat fluxes are discovered in certain depths. In Bryn this effect is proven to be due to groundwater flow in the upper 20 m of the well and the same effect is likely to appear in limestone rocks (Lysaker and Raufoss) where pipeflow can occur (karst). The well reports from the well field at Nordstrand indicate a high probability of groundwater flow between 112 and 140 m where water flows larger than $1\,000\text{ l hr}^{-1}$ were measured during drilling.

Connected fracture networks may allow for a significant groundwater flow if a remarkable hydraulic gradient is present in the influence area.

A higher quartz content in different layers may have an influence on the heat flow and temperature recovery as well. A numerical simulation may provide an answer if changes in the rock type along the borehole play a more important role for the temperature recovery than the influence of groundwater.

c) Delta temperature profiles

Another possibility to interpret the temperature profile four hours after a TRT is to compare it with the temperature profile before a TRT by subtracting the two from each other:

$$\Delta T(z) = T_{4hr}(z) - T_{ini}(z)$$

where $T_{4hr}(z)$ temperature measured 4 hr after TRT at depth z
 $T_{ini}(z)$ temperature measured before TRT at depth z

The assumptions that should be fulfilled for comparison of ΔT profiles at different sites are:

- a) all TRTs have been performed with the same heating power
- b) all boreholes have the same effective depth (i.e. the water saturated part)
- c) all TRTs have been performed for the same period of time
- d) temperature profiles have been measured exactly four hours after the TRT following an identical measurement procedure
- e) the rock is homogeneous and isotropic
- f) no groundwater flow is present

If all assumptions are fulfilled in the experiment, the ΔT value should be largest if the thermal conductivity of the ground is poor, e.g. the temperature cannot recover as fast as in a rock with high thermal conductivity.

For a visual comparison, ΔT profiles were chosen that fulfill at least assumptions a) to d) (Smestad, Raufoss, Fredrikstad and Modum). All of the TRTs have been performed with 6 kW power for the heating elements (assumption a)). The effective depth was similar (187 – 196 m, assumption b)). All TRTs have been performed for approximately the same time (71.17 to 71.83 hours, assumption c)) and an identical measurement scheme was followed for

all temperature profiles (assumption d)). Assumptions e) and f) are not fulfilled but the importance of these factors may be shown through such a comparison.

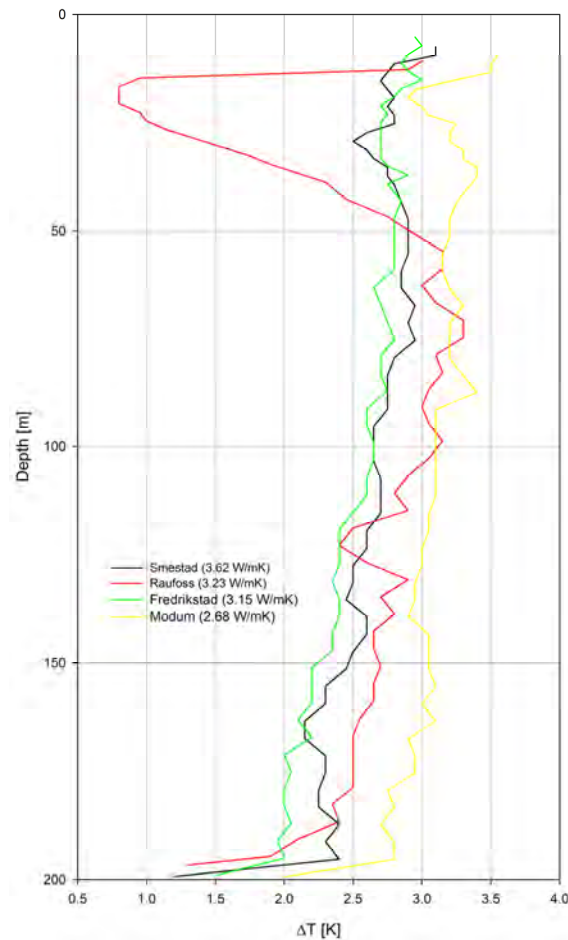


Fig. 3.12: Delta temperature profiles for the 200 m deep wells at Smestad, Raufoss, Fredrikstad and Modum.

The ΔT profiles at Modum, Raufoss and Smestad show the expected result (Fig. 3.12). The temperature recovery is slowest (the ΔT highest) at the well where the lowest effective thermal conductivity was measured: Modum ($2.68 \text{ W m}^{-1} \text{ K}^{-1}$). In contrast, the fastest temperature recovery is found in Smestad where the highest effective thermal conductivity was measured ($3.62 \text{ W m}^{-1} \text{ K}^{-1}$). Raufoss shows an intermediate temperature recovery despite the remarkable influence of groundwater in the uppermost 50 m.

The ΔT profile at Fredrikstad shows a temperature recovery faster than at any of the other wells even if the measured effective thermal conductivity shows an intermediate value similar to the one from Raufoss. As the ΔT profile does not contain strong deviations and the assumptions are fulfilled in the same way as for the other wells, no good explanation has been found so far.

d) Geothermal gradients

All temperature profiles of this investigation are presented in Fig. 3.13. They are shown depending to their altitude above sea-level. The dataset has been supplemented with one extra temperature profile taken at Slemmestad (32N, 583076 E, 6627511 N, 10.08.2009). Theoretically, their upper boundary temperature should increase by $0.65\text{ }^{\circ}\text{C} / 100\text{ m}$ due to the standard adiabatic temperature gradient of the troposphere. Again, this effect is overprinted by local factors (shade, albedo of the surface, topography, buildings...) and distance to the sea.

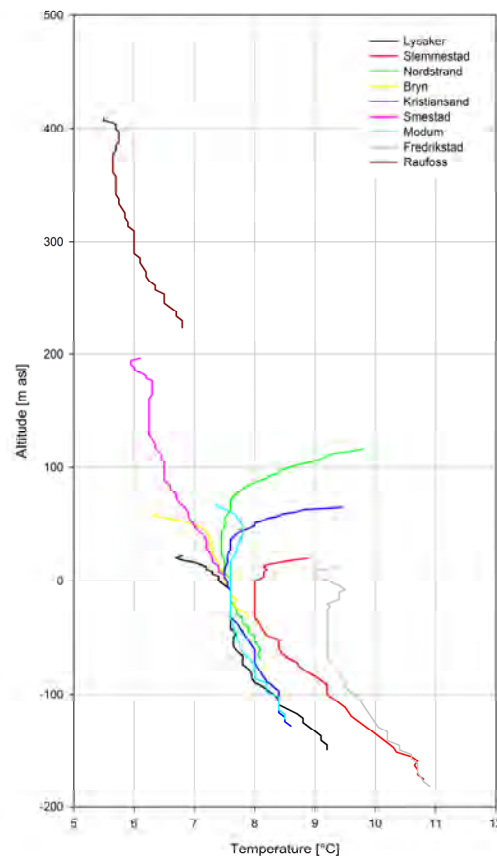


Fig. 3.13: Temperature profiles according to their elevation of all well of this investigation plus one profile at Slemmestad.

The topography has an effect on the heat flow in the ground as well. The temperature gradient should be lower below a hill than below a valley (Midttømme, 2000). Slope orientation and inclination of a hillside are further aspects that affect heat flow (Blackwell et al., 1980). Topography effects have to be expected in the temperature profiles of this study and taken into consideration for their interpretation.

Visually, the temperature profiles at Slemmestad and Fredrikstad differ from other profiles taken in the Oslo region.

The temperature profile at Fredrikstad shows a similar geothermal gradient as for Slemmestad but the overall temperature in the ground is considerably higher. The surface temperature is rather high because of the southerly position close to the Skagerrak which prevents cold winters and gives a milder climate than in the inner Oslofjord area. In addition, the borehole is drilled at a south-facing hillside. The high temperature in the ground may be explained with the high heat production of the Iddefjord granite. A value of $6.3 \mu\text{W m}^{-3}$ for the latter rock type (Slagstad et al., 2009) opposes a value of $1.5 \mu\text{W m}^{-3}$ for basement rocks of the inner Oslofjord area (Midttømme, 2000).

At Slemmestad the situation is different. The well is located between a small forest and a soccer ground. The average air temperature at that site might be considerably lower than at Fredrikstad. Even if Lower Ordovician shales crop out at the surface, the well report indicates a change in the colour of the ground rock towards “dark grey” below 87 meters. This is likely the border with Cambrian alum shales that are known to contain a high amount of radioactive elements belonging to the Uranium-Lead decay series. In alum shales in the Oslo region heat production values were measured as high as $30.6 \mu\text{W m}^{-3}$ (Slagstad et al., 2009). This in combination with the vicinity to the Precambrian basement which might as well show a higher heat production than the Cambro-Silurian limestones and shales, might explain the highest geothermal gradient of this investigation of $21.1 \text{ }^\circ\text{C km}^{-1}$ (calculated from the temperature profile between 100 and 200 m depth).

Generally, the geothermal gradients vary considerably between the sites (see Table 3.3).

Table 3.3: Geothermal gradients [$^\circ\text{C km}^{-1}$] at the different sites calculated from the temperature profiles for depths below 100 m.

Site	Geothermal gradient [$^\circ\text{C km}^{-1}$]
Modum	4.6
Nordstrand	7.0
Kristiansand	9.3
Smestad	9.8
Raufoss	9.9
Fredrikstad	14.8
Lysaker	18.3
Slemmestad	21.1

The attempt to correlate the effective thermal conductivity to the measured geothermal gradients in the different wells was not successful. It seems that the temperatures measured down to 200 m do not always represent an undisturbed characteristic geothermal gradient

because of different reasons discussed above (paleoclimate, changing thermal conductivities in different rock layers). This problem can be partly overcome if deeper boreholes are studied.

e) Influence of buildings

At "Nordstrand videregående skole" an energy well field was drilled in spring 2009. A standard TRT was performed in borehole 3 (Bh3, see Fig. 3.14).

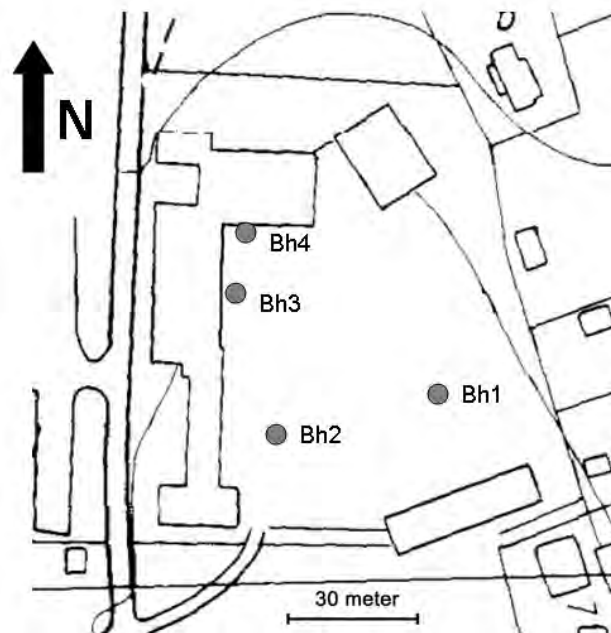


Fig. 3.14: Map over "Nordstrand videregående skole" and position of boreholes (Bh) where temperature profiles were measured (map taken from Statens kartverk, 2009, mod.).

The temperature profile before the TRT showed surprisingly high ground temperatures down to at least 40 m. Three other available wells were chosen to take temperature profiles. Based on the effective thermal conductivity measured in the ground heat flow profiles were calculated.

Fig. 3.15 shows the strongest heat flow from the surface towards the ground in the borehole closest to the main school building. The school building was built 1926 and influences the temperature profiles down to 60 m depth in the direct vicinity of the building.

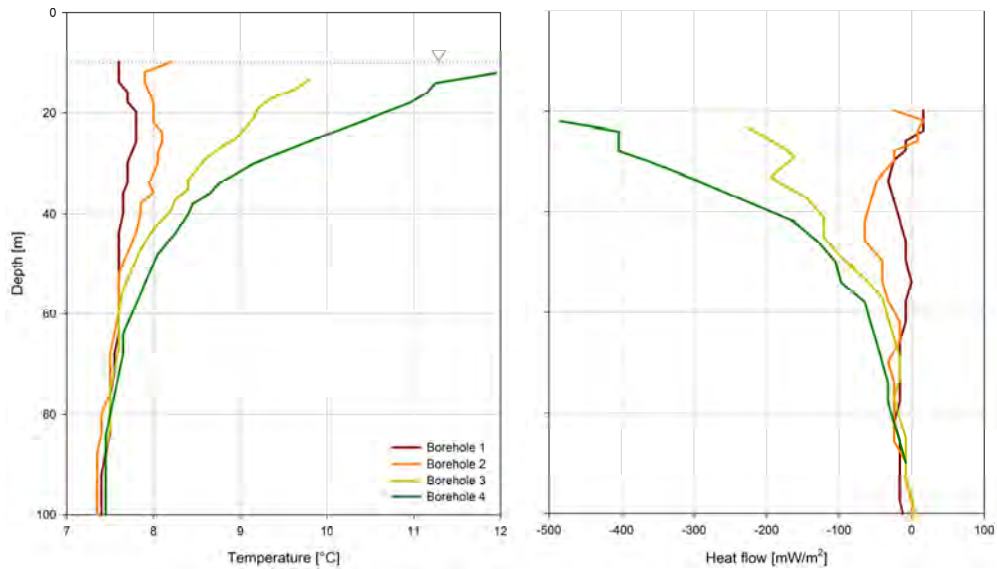
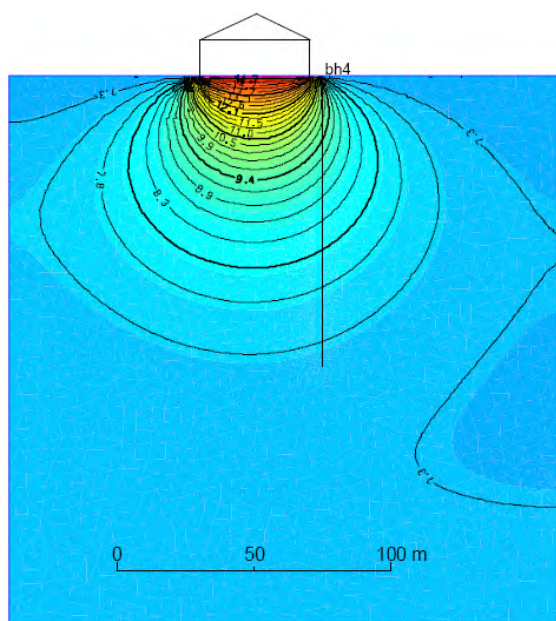


Fig. 3.15: Temperature profiles (left) and heat flow (right) (20 meter intervals used for calculations) in four boreholes at Nordstrand. The dotted line and the triangle show the groundwater level.

The same phenomenon was described as well for a building in Cambridge (Massachusetts, USA) where the influence was modelled to be down to almost 150 m, 50 years after the construction of the building (Roy et al., 1972). Roy and colleagues modelled the underground heat plume defining a Dirichlet temperature boundary condition for the building which was set to 15 °C. This strategy was taken over in a simple two-dimensional FE model for the thermal plume at Nordstrand school. The model was built up in FEFLOW 5.4 (DHI-WASY GmbH, Berlin, Germany).



Model parameter

Thermal conductivity	3.23 K W ⁻¹ m ⁻¹
Porosity	0.05
Geothermal gradient	7 K km ⁻¹
Simulation time	29930 d

Fig. 3.16: Simulated heat plume below Nordstrand school 82 years after the construction.

The effect of heat loss towards the ground depends among others on the insulation of the building, the thermal conductivity of the ground and the presence of groundwater flow. The results of the simulation (Fig. 3.16) fit very well with the temperature profile taken at borehole 4 (Fig. 3.15). The model is based on the assumption that no groundwater flow appeared during the simulation period and that the rock is homogeneous and isotropic. Even if the geological outcrops at the surface indicate that there is a thermal anisotropic behaviour, the effect might be neglectable if the orientation of the foliation in the gneisses changes with depth.

A mathematical description of the heat loss phenomenon from buildings towards the ground is given in Hagentoft (1996a,b).

4. GLOBAL EVALUATION

4.1 BRYN

1) Groundwater significantly influences the effective thermal conductivity in hard rock aquifers measured with a TRT.

The data of the TRTs with and without pumping of groundwater at Bryn confirm the hypothesis. Considering the draw-down of the groundwater table of almost four meters during pumping of groundwater from a nearby well, the difference in the effective thermal conductivity with an increase of $0.4 \text{ W K}^{-1}\text{m}^{-1}$ with groundwater flow is lower than expected. It is difficult to estimate a realistic hydraulic transmissivity for the fractured aquifer. Therefore, more TRTs with pumping of groundwater should be done in fractured aquifers with a more regular fracture pattern where standard hydrogeological analyses can be applied (e.g. the Warren and Root model, 1963). Both geological and hydrogeological parameters then can be determined easier. Investigation areas with a well understood natural groundwater flow are a possible alternative.

II) Lateral groundwater flow can be detected in temperature profiles after a TRT.

The hypothesis could be confirmed *via* temperature profiles carried out four hours after the finishing of a TRT in Bryn and at other locations as well (e.g. Nordstrand, Raufoss). Well-sections that show groundwater flow are characterized by a remarkably faster temperature recovery after the TRT as heat is transported away from the well. The mineral content of different geological layers seems to have a less pronounced influence on the temperature recovery.

4.2 OSLO REGION

I) Effective thermal conductivity values measured via TRTs in the Oslo region (non-grouted, water-filled boreholes) are higher than the lab measured thermal conductivity from rock cores.

Effective thermal conductivity data measured in this study does not show a trend towards higher thermal conductivity values in comparison to lab measured thermal conductivity values from rock cores. Expanding the dataset however with all available data of TRTs performed in the Oslo region by other companies confirms the hypothesis.

The deviation from the rock core samples, however, can be very high due to the fact that several geological layers may be represented in one single well. Furthermore, the rock core samples vary as well within the same geological unit. The best solution would be to use rock samples from different depths of the borehole in which the TRT is performed. The drilling costs of a continuous rock core for a complete well are too high, however.

II) Thermal conductivity maps (like the one of Ramstad et al. 2008b) based on surface rock core data can replace TRTs.

So far gathered data from TRTs performed in the Oslo region and the comparison with the rock core sample data indicate that there is too much variation in both measurements to base the planning of a large ground-source heat project only on a thermal conductivity map based

on rock core measurements. The thermal conductivities from rock cores give only spotlight data for single outcrops of different rocks belonging to one geological unit.

The statistical analysis depicts that TRTs in metamorphic rocks show thermal conductivities more similar to those measured in the lab while effective thermal conductivity values are by trend higher than thermal conductivity values from sedimentary and igneous rock core samples. The comparison of both thermal conductivity measurements does not give a clear answer for the question how much higher the *in situ* thermal conductivity is at a location in comparison to the data from rock cores of the geological unit. The standard deviation within both TRT and rock core thermal conductivity data for all different geological units or rock types are higher than the differences between their mean values for a geological unit.

This indicates that the planning of a large ground-source heat project cannot be based on a thermal conductivity map only without analysing the *in situ* geological and hydrogeological conditions.

All effective thermal conductivity data from TRTs performed at the Oslo region should be collected to allow for improved statistical analyses based on a larger dataset and for statistical comparisons between TRT and rock core data of further geological units.

4.3 FURTHER WORK AND RECOMMENDATIONS

The data collected during this field study show that groundwater has a considerable influence on the TRT results in fractured aquifers. At Bryn a coupled groundwater flow – heat transport finite element model will be built up to quantify the influence of groundwater on TRTs. The model can be calibrated and validated with the field data collected at Bryn in this and former studies. Furthermore, the model can be used to find the best timing to perform a temperature profile after a TRT to have the best possibilities to discover groundwater flow at the investigation well. It might even be possible to estimate the part of the effective thermal conductivity which is caused by the lateral groundwater flow directly from the temperature profile after the TRT. In addition, the model should take into consideration varying mineral compositions in different layers as they have an influence on the heat flow and temperature recovery as well. A numerical simulation may answer if changes in the rock type along the borehole are neglectable for the temperature recovery in comparison to the influence of groundwater.

Based on the results so far, it is recommended to carry out standardized temperature profiles before and four hours after the TRT to gain information about varying thermal conductivities along the borehole due to inhomogeneous mineral content and groundwater flow along fractures. The temperature profiles should be a standard code of practice in any thermogeological pre-investigation of a larger ground-source heat project as only a realistic effective thermal conductivity allows for a secure modeling of the required effective borehole length to run a ground-source heat pump efficiently.

5. CONCLUSIONS

- Groundwater flow in fractured aquifers enhances the effective (*in situ*) thermal conductivity.
- Groundwater flow can be discovered easily by the comparison of standardized temperature profiles before and after a TRT.
- ΔT profiles help to visualize groundwater flow and varying mineral content with different thermal properties (e.g. quartz-rich layers).
- Varying thermal properties of the ground can be discovered and interpreted based on standardized temperature profiles before and after a TRT.
- Water and alcohol as collector fluid give identical TRT results for both borehole resistance and effective thermal conductivity.
- Effective thermal conductivity values are in average significantly higher than lab-measured thermal conductivity values from rock cores.
- Thermal conductivities measured *via* TRTs are significantly higher than in rock core samples in syenite and Silurian and Ordovician sediments while no significant difference could be found in gneisses.
- The thermal conductivity ratio $\lambda_{\text{eff}} / \lambda_{\text{rockcore}}$ in metamorphic rocks is close to 1.0 and significantly lower than in igneous and sedimentary rocks.
- Thermal conductivity maps based on rock cores cannot replace TRTs as thermogeological pre-investigation for larger ground-source installations.
- Buildings built about 80 years ago can change the underground temperature distribution down to at least 100 m depth.

- Thermal gradients at the first 100 m depth are dominated by surface temperature changes (e.g. exposition, slope, albedo, shade, buildings, etc.)
- Realistic geothermal gradients are not obtained in the uppermost 200 m of the crust as several factors alter the underground temperature (paleoclimate effects, groundwater flow, varying heat production in different rocks, etc.)

6. ACKNOWLEDGMENTS

The authors are thankful for the synergetic cooperation with Bjørn Borgnes (Futurum Energi AS) and John Ihlen (Båsum Boring Oslo AS). Helge Skarphagen (Norsk institutt for vannforskning NIVA) helped to get started the groundwater pump at Bryn. Valuable comments were given by Allan Krill (professor in geology at NTNU). The study was financed by the Norwegian University of Science and Technology (NTNU) and the Geological Survey of Norway (NGU).

7. LITERATURE

- Banks, D., M.L. Solbjørg, E. Rohr-Torp (1992a): Permeability of fracture zones in a Permian granite. *Quarterly Journal of Engineering Geology* 25: 377-388.
- Banks, D., E. Rohr-Torp, H. Skarphagen (1992b): An integrated study of a Precambrian granite aquifer, Hvaler, Southeastern Norway. *Geological Survey of Norway, Bulletin* 422: 47-66.
- Banks, D., E. Rohr-Torp, H. Skarphagen (1994): Groundwater resources in hard rock; experiences from the Hvaler study, southeastern Norway. *Applied Hydrogeology* 94: 33-42.
- Banks, D. (2008): *An introduction to thermogeology – Ground source heating and cooling*. Blackwell Publishing Ltd., Oxford, UK.
- Barenblatt, G.I., P. Zheltov, N. Kochina (1960): Basic concepts in the theory of seepage of homogeneous liquids in fissured rocks. *Prikl. Mat. Mekh.*, 24: 852-864.
- Blackwell, D.D., J.L. Steele, C.A. Brott (1980): The terrain effect on terrestrial heat flow. *Journal of Geophysical Research* 85: 4757–4772.
- Boge, K., T. Åndal, R. Kjølberg (2002): Final report for the pregrouting at the T-baneringen tunnel (stage one, Ullevål-Nydalen). Norwegian Public Roads Administration, Tunnels for the citizens, Report No. 16, pp. 28.
- Campbell, C. and J. Laherrère (1998): The end of cheap oil. *Scientific American* 278: 78-83.
- Clauser, C. and E. Huenges (1995): Thermal conductivity of rocks and minerals. In: T.J. Ahrens (ed.): *Rock physics and phase relations – A handbook of physical constants*. American Geophysical Union, Washington, USA.
- Chiasson, A. D., S. J. Rees, J.D. Spitler (2000): A preliminary assessment of the effects of groundwater flow on closed-loop ground source heat pump systems, United States, American Society of Heating, Refrigerating and Air-Conditioning Engineers, Inc., Atlanta, GA (US); Oklahoma State Univ., Stillwater, OK (US).
- Davies, N.S., P. Turner, I.J. Sansom (2005): A revised stratigraphy for the Ringerike Group (Upper Silurian, Oslo Region). *Norwegian Journal of Geology* 85: 193-201.
- Domenico, P.A. and F.S. Schwartz (1998): *Physical and Chemical Hydrogeology*. John Wiley & Sons Inc., New York, USA.
- Dons, J.A., J.F. Bockelie, I. Bryhni, G. Henningsmoen, J. Naterstad, O. Nilsen (1996): Oslo-traktenes geologi med 25 turbeskrivelser. Vett & Viten AS, Nesbru, Norway.
- Earth Energy Designer v. 2.0 (2000): PC software for borehole heat exchanger design. Developed by T. Blomberg, J. Claesson, P. Eskilson, G. Hellström, B. Sanner.

- Ericsson, L. O. (1985): Värmeutbyte mellan berggrund och borrhål vid bergvärme-system. Department of Geology, Chalmers University of Technology and University of Göteborg, Sweden.
- Enova (2007): Fornybar energi. Private publishing, pp. 181. Online: <http://www.enova.no/file.axd?fileID=11> [25.11.2009].
- Fan, R., Y. Q. Jiang, Y. Yao, D. Shiming, Z.L. Ma (2007): A study on the performance of a geothermal heat exchanger under coupled heat conduction and groundwater advection. *Energy* 32: 2199-2209.
- Falkum, T. (1972): On large-scale tectonic structures in the Agder-Rogaland region, southern Norway. *Norwegian Journal of Geology* 52: 371-376.
- Fujii, H., R. Itoi, J. Fujii, Y. Uchida (2005): Optimizing the design of large-scale ground-coupled heat pump systems using groundwater and heat transport modeling. *Geothermics* 34(3): 347-364.
- Fujii, H., T. Inatomi, R. Itoi, Y. Uchida (2007): Development of suitability maps for ground-coupled heat pump systems using groundwater and heat transport models. *Geothermics* 36: 459-472.
- Gehlin, S. (1998): Thermal response test. In situ measurements of thermal properties in hard rock. Licentiate thesis. Luleå University of Technology, 1998:37.
- Gehlin, S. (2002): Thermal response test. Method development and evaluation. Doctoral thesis. Luleå University of Technology, 2002:39.
- Gehlin, S.E.A. and G. Hellström (2003): Influence on thermal response test by groundwater flow in vertical fractures in hard rock. *Renewable Energy* 28: 2221-2238.
- Gehlin, S.E.A., G. Hellström, B. Nordell (2003): The influence of the thermosiphon effect on the thermal response test. *Renewable Energy* 28: 2239-2254.
- Graversen, O. (1984): Geology and structural evolution of the Precambrian rocks of the Oslofjord-Øyeren area, southeast Norway. Geological Survey of Norway, Bulletin 398: 1-49.
- Gustafsson, A.M. (2006): Thermal Response Test – Numerical simulations and analyses. Licentiate thesis. Luleå University of Technology, 2006:14.
- Hagentoft, C.E. (1996a): Heat losses and temperature in the ground under a building with and without ground water flow—I. Infinite ground water flow rate. *Building and Environment* 31: 3-11.
- Hagentoft, C.E. (1996b): Heat losses and temperature in the ground under a building with and without ground water flow—II. Finite ground water flow rate. *Building and Environment* 31: 13-19.
- Holtedahl, O. (1953): Norges geologi. Bind I. Aschehoug & Co. Oslo, Norway.

- Ingersoll, L.R. (1948): Heat conduction – With engineering and geological application. McGraw-Hill Book Company, New York, USA.
- Jiang, Y. F. and A. D. Woodbury (2006): A full-Bayesian approach to the inverse problem for steady-state groundwater flow and heat transport. *Geophysical Journal International* 167: 1501-1512.
- Katsura, T., K. Nagano, S. Takeda, K. Shimakura (2006): Heat transfer experiment in the ground with ground water advection. *Proceedings of Ecostock 2006*, conference in New Jersey, USA, 31 May – 02 June, pp. 7.
- Katsura, T. (2009): Evaluation method of groundwater velocity applying the gradient of thermal response. *Proceedings of Effstock 2009*, conference in Stockholm, Sweden, 14-17 June, pp. 8.
- Kukkonen, I.T., W.D. Gosnold, J. Šafanda (1998): Anomalously low heat flow density in eastern Karelia, Baltic Shield: a possible paleoclimatic signature. *Tectonophysics* 291: 235-249.
- Larsen, B. (2001): Bryn skole, Bærum. Strukturgeologiske observasjoner. Unpublished, Geological Survey of Norway, pp. 3.
- Lee, C.K. and H.N. Lam (2009): Determination of groundwater velocity in thermal response test analysis. *Proceedings of Effstock 2009*, conference in Stockholm, Sweden, 14-17 June, pp. 8.
- Lewis, T.J. and K. Wang (1992): Influence of terrain on bedrock temperatures. *Palaeogeography, Palaeoclimatology, Palaeoecology* 98: 87-100.
- Løset, F. (1981): Geological engineering experience from the sewage tunnel Lysaker – Slemmestad. *Rock Blasting Conference*, Norwegian Tunneling Association, Oslo, 1-31 November, pp. 31.
- Løset, F. (2002): *Geology of the Norwegian tunnels*. Norwegian Geotechnical Institute, pp. 90.
- Lutro, O. and Ø. Nordgulen (2004): *Oslofeltet, berggrunnskart M 1:250 000*. Geological Survey of Norway.
- Lutro, O. and Ø. Nordgulen (2008): *Oslofeltet, berggrunnskart M 1:250 000*. Geological Survey of Norway.
- Middleton, M.F. (1993): A transient method of measuring the thermal properties of rocks. *Geophysics* 58: 357-365.
- Midttømme, K. (2000): *Temperaturgradienter, varmemestrøm og radioaktiv energi i Osloområdet*. Geological Survey of Norway, Report 2000.006.
- Midttømme, K. (2005): Norway's geothermal energy situation. *Proceedings World Geothermal Congress 2005, Antalya, Turkey, 24.-29.04.*, pp. 5.

- Midttømme, K., R. K. Ramstad, A. Solli, T. Sjørdal, H. Elvebakk (2004): Grunnvarmekartlegging i Asker og Bærum. Geological Survey of Norway, Report 2004.013.
- Morland, G. (1997): Petrology, lithology, bedrock structures, glaciation and sea level. Important factors for groundwater yield and composition of Norwegian bedrock boreholes? Geological Survey of Norway, Report 97.122.
- Naterstad, J., J. Bockelie, J.F. Bockelie, O. Graversen, H. Hjelmeland, B.T. Larsen, O. Nilsen (1990): Asker 1814 I, berggrunnskart M 1:50 000. Geological Survey of Norway.
- Nordstrand, J.S. (2001): Energibrønner i fjell - Vurdering av forskjellige metoder for effektuttak ved et demonstrasjonsanlegg. Master thesis at the Norwegian University of Science and Technology, Department of Geology and Mineral Resources, pp. 72.
- Olesen, O., J.F. Dehls, J. Ebbing, H. Henriksen, O. Kihle, E. Lundin (2006): Aeromagnetic mapping of deep-weathered fracture zones in the Oslo Region – a new tool for improved planning of tunnels. *Norwegian Journal of Geology* 87: 253-267.
- Opalinski, P.R., T.L. Harland (1981): The Middle Ordovician of the Oslo Region, Norway, 29. Stratigraphy of the Mjøsa Limestone in the Toten and Nes-Hamar areas. *Norwegian Journal of Geology* 61: 59-78.
- Pannike, S., M. Koelling, B. Panteleit, J. Reichling, V. Scheps, H.D. Schulz (2006): Influence of hydrogeological parameters on temperature variations due to borehole heat exchangers. *Grundwasser* 11: 6-18.
- Pedersen, S. and S. Maaloe (1990): The Iddefjord granite: geology and age. Geological Survey of Norway, Bulletin 417: 55–64.
- Ramberg, I.B., I. Bryhni, A. Nøttvedt (2006): Landet blir til – Norges geologi. Geological Society of Norway, Trondheim, Norway.
- Ramstad, R. K. (2004): Ground source energy in crystalline bedrock – increased energy extraction by using hydraulic fracturing in boreholes. Doctoral Theses at NTNU 2004: 161.
- Ramstad, R.K., B.O. Hilmo, B. Brattli, H. Skarphagen (2007): Ground source energy in crystalline bedrock-increased energy extraction using hydraulic fracturing in boreholes. *Bulletin of Engineering Geology and the Environment* 66: 493-503.
- Ramstad, R.K., H. de Beer, K. Midttømme, J. Koziel, B. Wissing (2008a): Thermal diffusivity measurement at NGU – Status and method development 2005-2008. Geological Survey of Norway, Report 2008.050
- Ramstad, R.K., H. Tiarks, K. Midttømme (2008b): Ground source energy – Thermal conductivity map in the Oslo region. Poster shown at NGU's stand at the 33rd International Geologic Congress Oslo, August 6-14th.
- Rohr-Torp, E. (1973): Permian Rocks and Faulting in Sandsvær at the Western Margin of the Oslo Region. Geological Survey of Norway, Report 73.300: 53-71.

- Rohr-Torp, E. (1994): Present uplift rates and groundwater potential in Norwegian hard rocks. Geological Survey of Norway, Bulletin 426: 47-52.
- Roy, R.F., D.D. Blackwell, E.R. Decker (1972): Continental heat flow. Chapter 19, in: *The Nature of the Solid Earth*, ed. E.C. Robertson, pp. 506-544. McGraw Hill, New York, USA.
- Sims, R.E.H., R.N. Schock, A. Adegbululgbé, J. Fenhann, I. Konstantinaviciute, W. Moomaw, H.B. Nimir, B. Schlamadinger, J. Torres-Martínez, C. Turner, Y. Uchiyama, S.J.V. Vuori, N. Wamukonya, X. Zhang (2007): Energy supply. In *Climate Change 2007: Mitigation. Contribution of Working Group III to the Fourth Assessment Report of the Intergovernmental Panel on Climate Change* [B. Metz, O.R. Davidson, P.R. Bosch, R. Dave, L.A. Meyer (eds)], Cambridge University Press, Cambridge, United Kingdom and New York, USA.
- Skjeseth, S. (1963): Contributions to the geology of the Mjøsa district and the classical sparagmite area in southern Norway. Geological Survey of Norway, Bulletin 220: 1-126.
- Slagstad, T., N. Balling, H. Elvebakk, K. Midttømme, O. Olesen, L. Olsen, C. Pascal (2009): Heat-flow measurements in Late Paleoproterozoic to Permian geological provinces in south and central Norway and a new heat-flow map of Fennoscandia and the Norwegian-Greenland Sea. *Tectonophysics* 473: 341-361.
- Statens kartverk (2009): Norgesglasset. Online: <http://ngis2.statkart.no/norgesglasset/default.html> [20.11.2009].
- Stern, N. (2006): *The Stern review report on the economics of climate change*. Cambridge University Press, UK.
- Time Magazine (2009): Global warming heats up. Online: <http://www.time.com/time/magazine/article/0,9171,1176980,00.html> [19.10.2009].
- Turcotte, D. L., G. Schubert (2002): *Geodynamics* (2 ed.). Cambridge University Press, Cambridge, UK, pp. 136–137.
- Warren, J.E. and P.J. Root (1963): The behaviour of naturally fractured reservoirs. *Journal of the Society of Petroleum Engineers*, 3: 245-256.
- Welt (2008): Treibhausgase – Höchste Konzentration seit 800 000 Jahren. Online: http://www.welt.de/wissenschaft/article1995358/Hoehste_Konzentration_seit_800_000_Jahren.html [14.05.2008].
- Witte, H. (2002): Ground thermal conductivity testing: Effects of groundwater on the estimate. Abstract. 3. Kolloquium des Arbeitskreises Geothermik der DGG, Aachen, Germany, 03.-04.10.

APPENDIX A: TRT data, Oslo region

Fredrikstad:

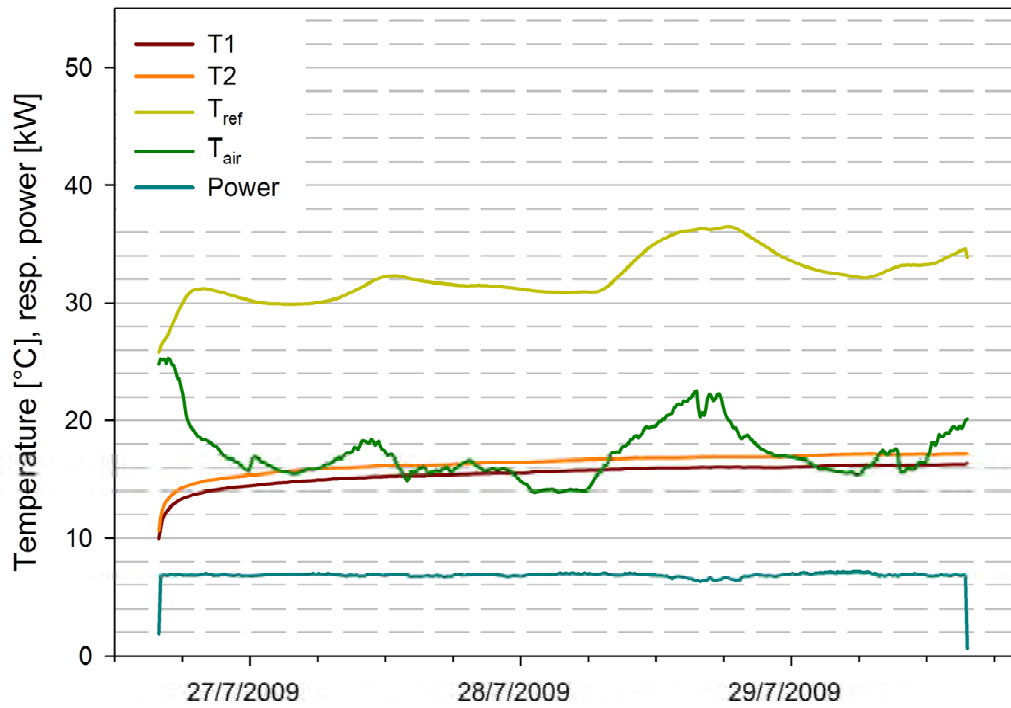


Fig. A1: TRT at Fredrikstad. T1: up-flow temperature, T2: down-flow temperature, T_{ref} : reference temperature inside the TRT trailer, T_{air} : ambient air temperature, Power: used for the heat elements and the circulation pump.

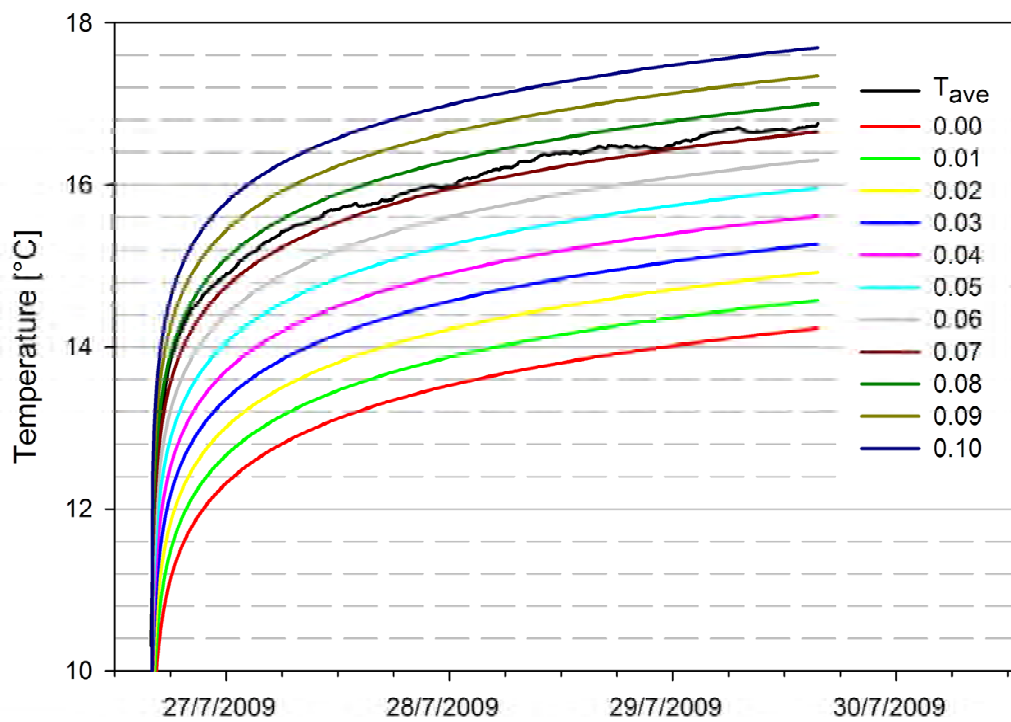


Fig. A2: Average fluid temperature in the collector (T_{ave}) and borehole resistance type curves [$K m W^{-1}$] at Fredrikstad.

Kristiansand:

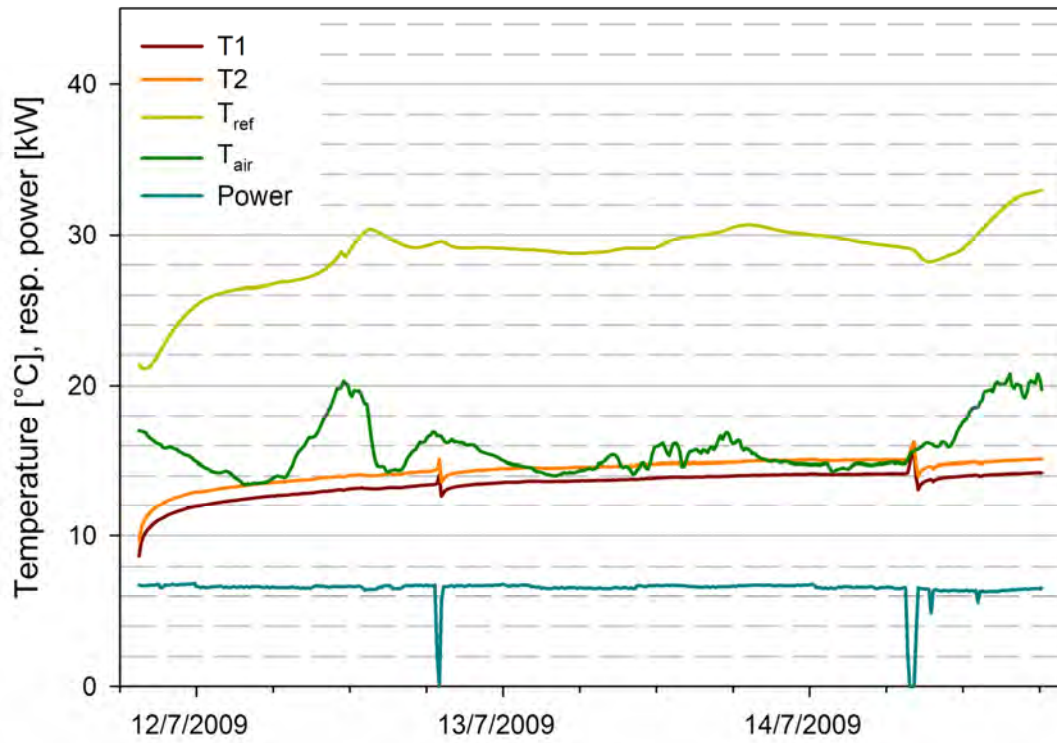


Fig. A3: TRT at Kristiansand. T1: up-flow temperature, T2: down-flow temperature, T_{ref} : reference temperature inside the TRT trailer, T_{air} : ambient air temperature, Power: used for the heat elements and the circulation pump.

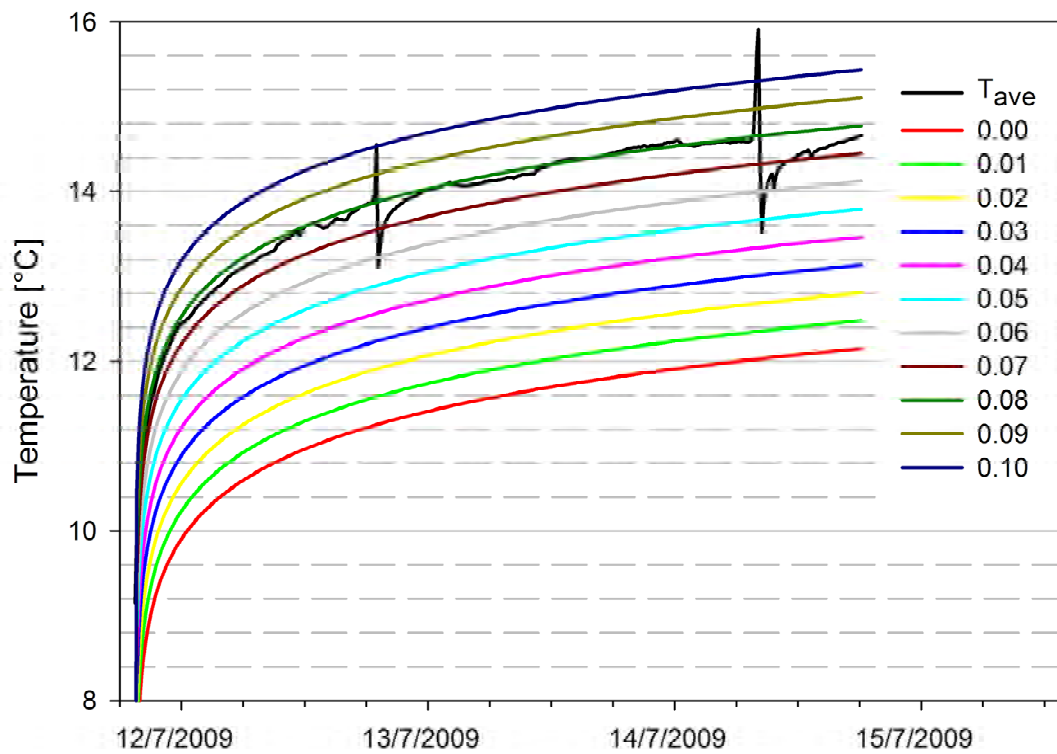


Fig. A4: Average fluid temperature in the collector (T_{ave}) and borehole resistance type curves [$K m W^{-1}$] at Kristiansand.

Lysaker:

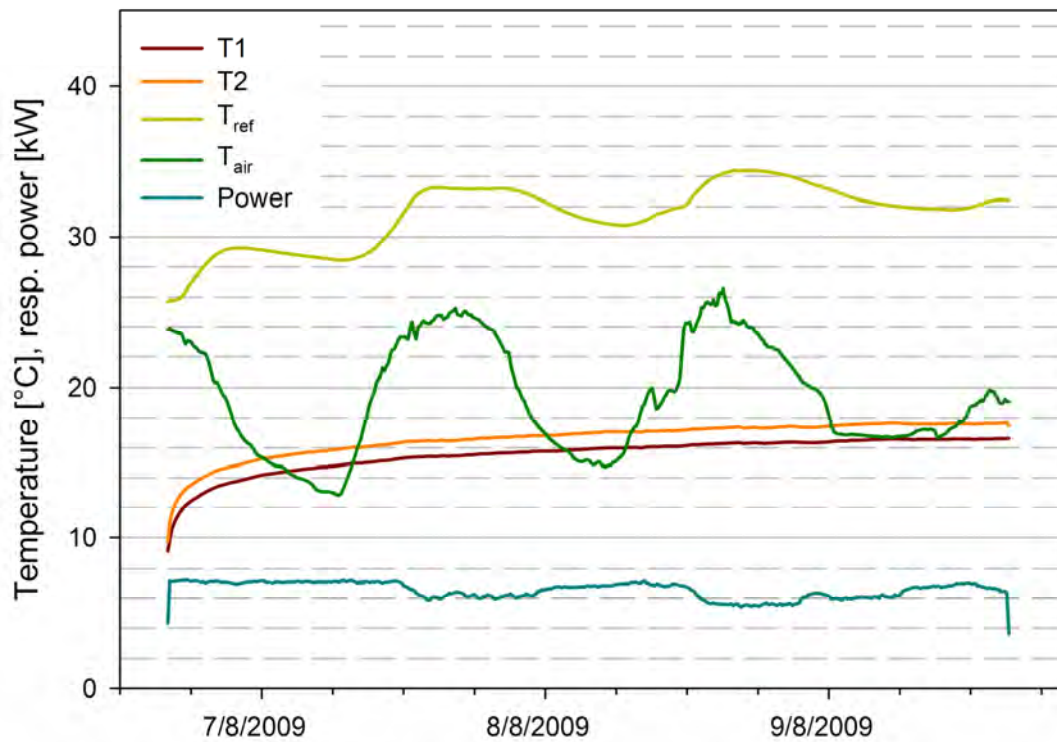


Fig. A5: TRT at Lysaker. T1: up-flow temperature, T2: down-flow temperature, T_{ref}: reference temperature inside the TRT trailer, T_{air}: ambient air temperature, Power: used for the heat elements and the circulation pump.

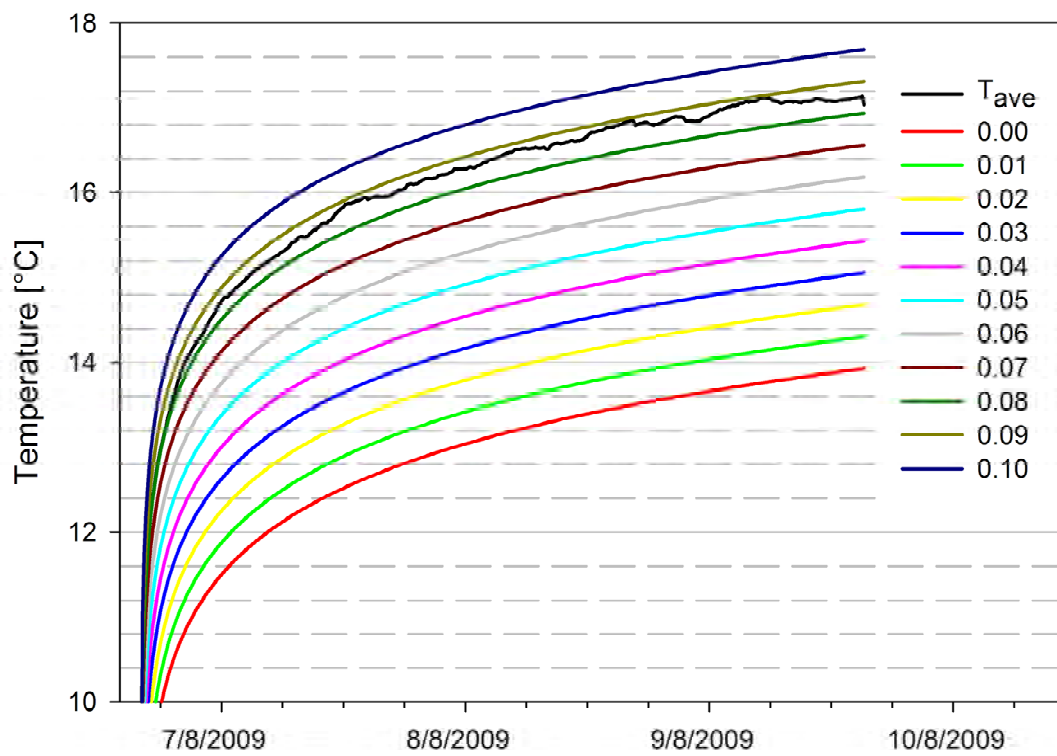


Fig. A6: Average fluid temperature in the collector (T_{ave}) and borehole resistance type curves [K m W⁻¹] at Lysaker.

Modum:

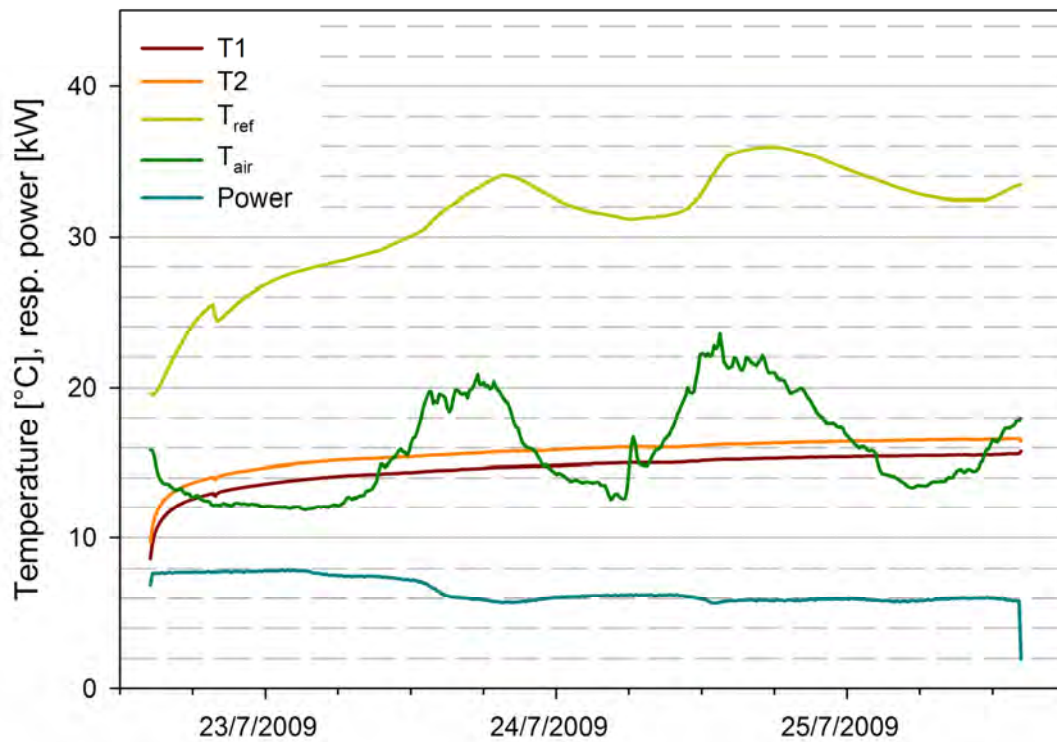


Fig. A7: TRT at Modum. T1: up-flow temperature, T2: down-flow temperature, T_{ref} : reference temperature inside the TRT trailer, T_{air} : ambient air temperature, Power: used for the heat elements and the circulation pump.

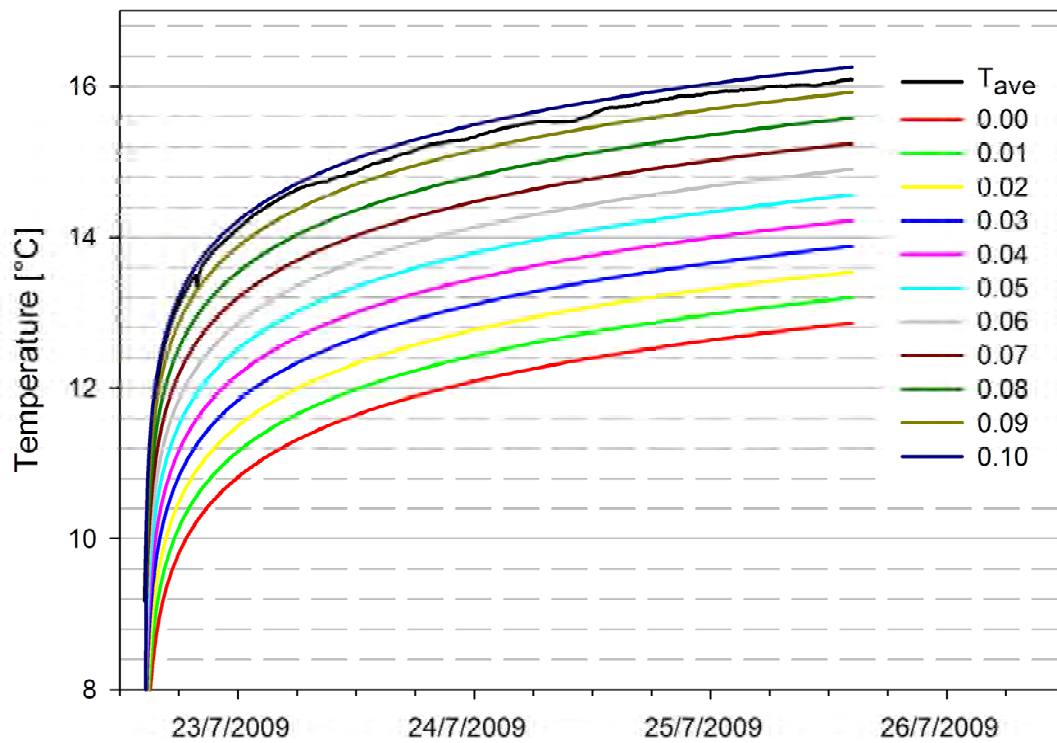


Fig. A8: Average fluid temperature in the collector (T_{ave}) and borehole resistance type curves [$K m W^{-1}$] at Modum.

Nordstrand:

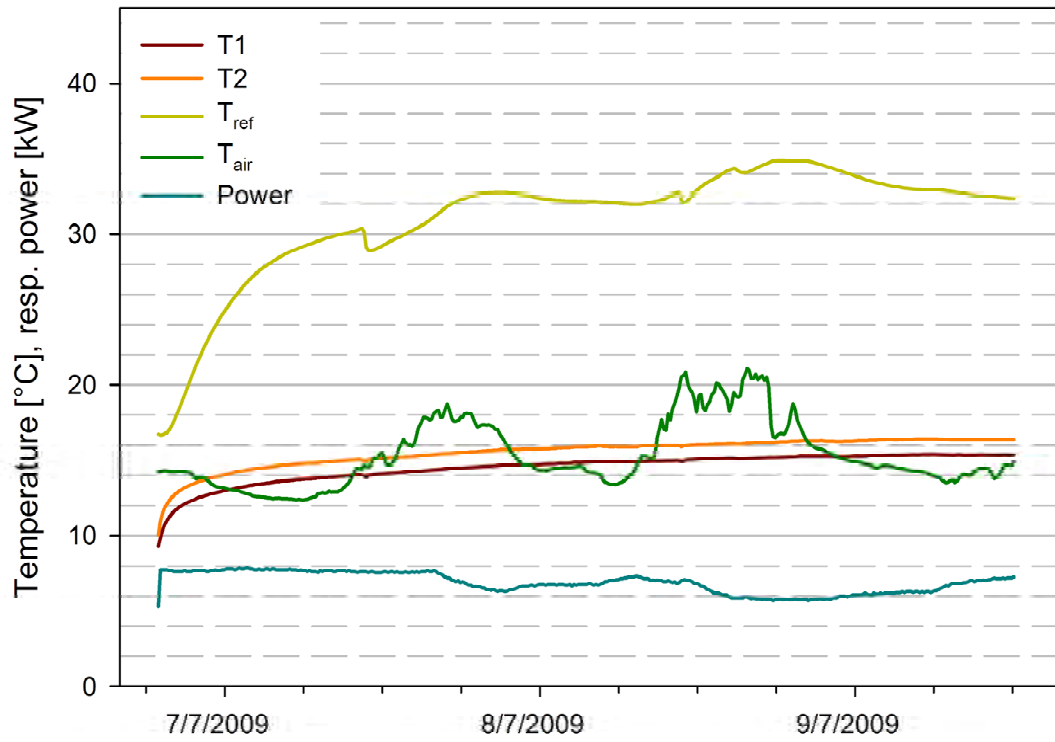


Fig. A9: TRT at Nordstrand. T1: up-flow temperature, T2: down-flow temperature, T_{ref} : reference temperature inside the TRT trailer, T_{air} : ambient air temperature, Power: used for the heat elements and the circulation pump.

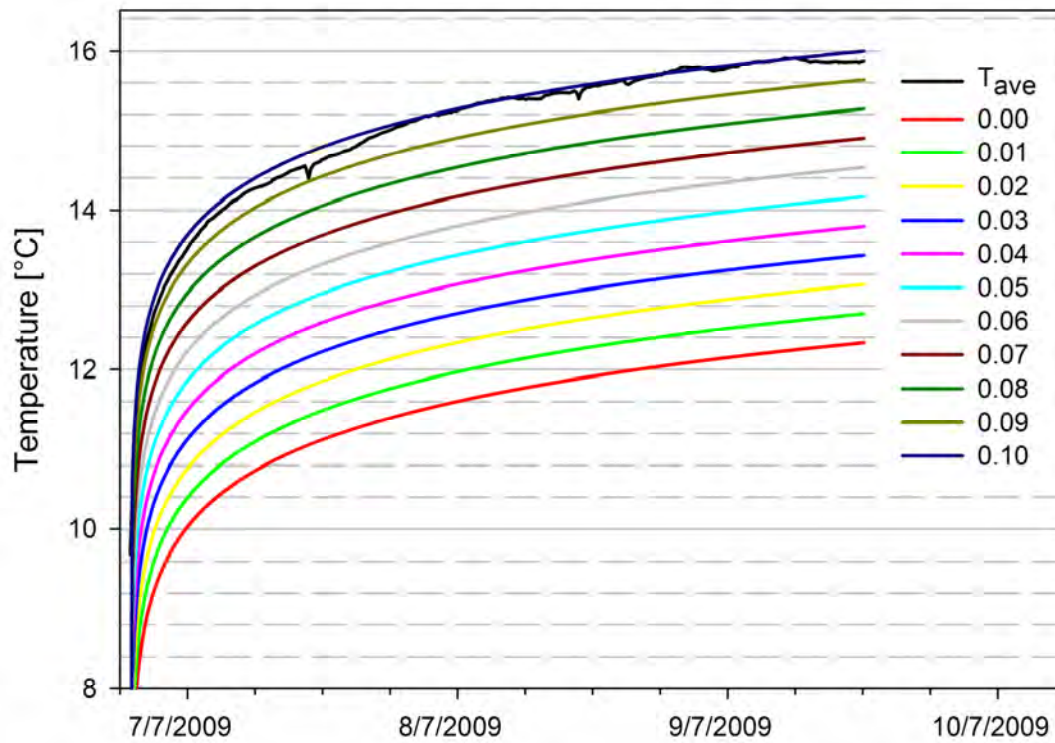


Fig. A10: Average fluid temperature in the collector (T_{ave}) and borehole resistance type curves [$K m W^{-1}$] at Nordstrand.

Raufoss:

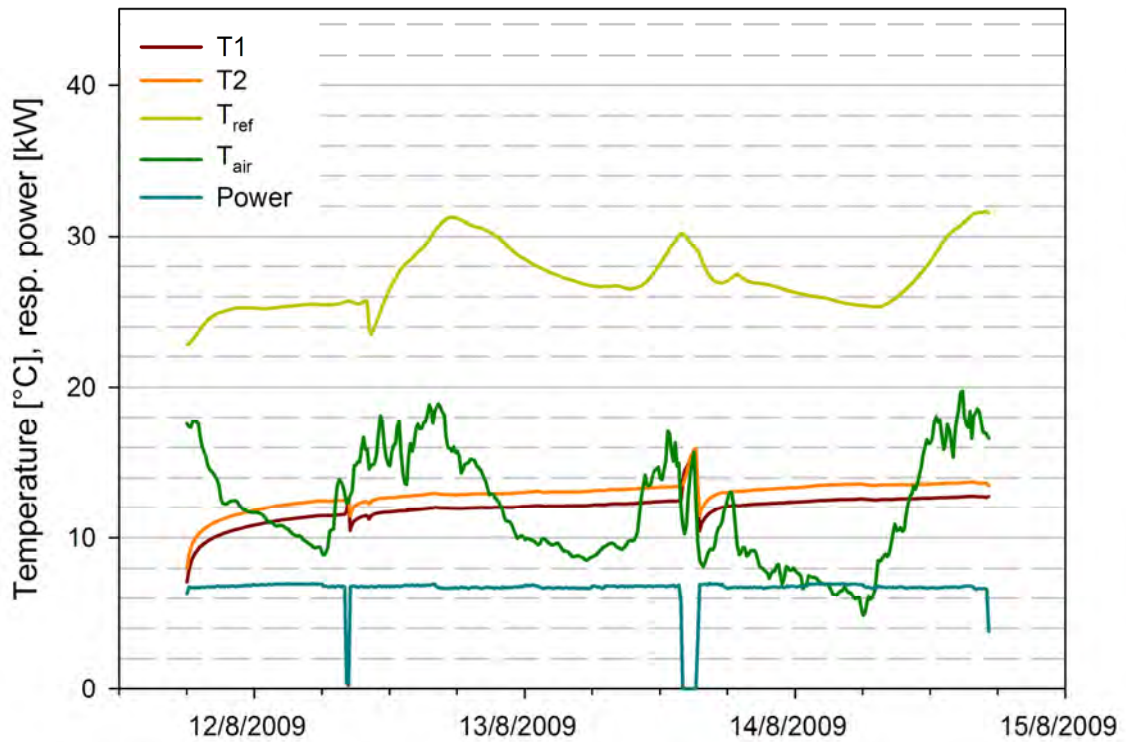


Fig. A11: TRT at Raufoss. T1: up-flow temperature, T2: down-flow temperature, T_{ref} : reference temperature inside the TRT trailer, T_{air} : ambient air temperature, Power: used for the heat elements and the circulation pump.

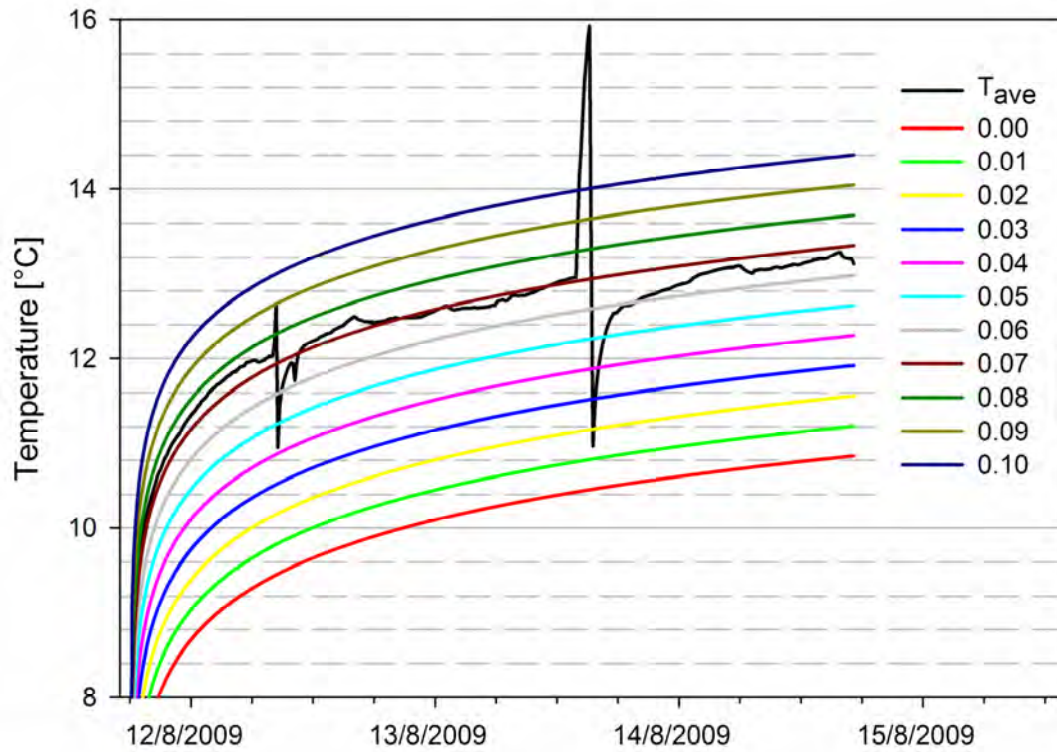


Fig. A12: Average fluid temperature in the collector (T_{ave}) and borehole resistance type curves [$K m W^{-1}$] at Raufoss.

Smestad:

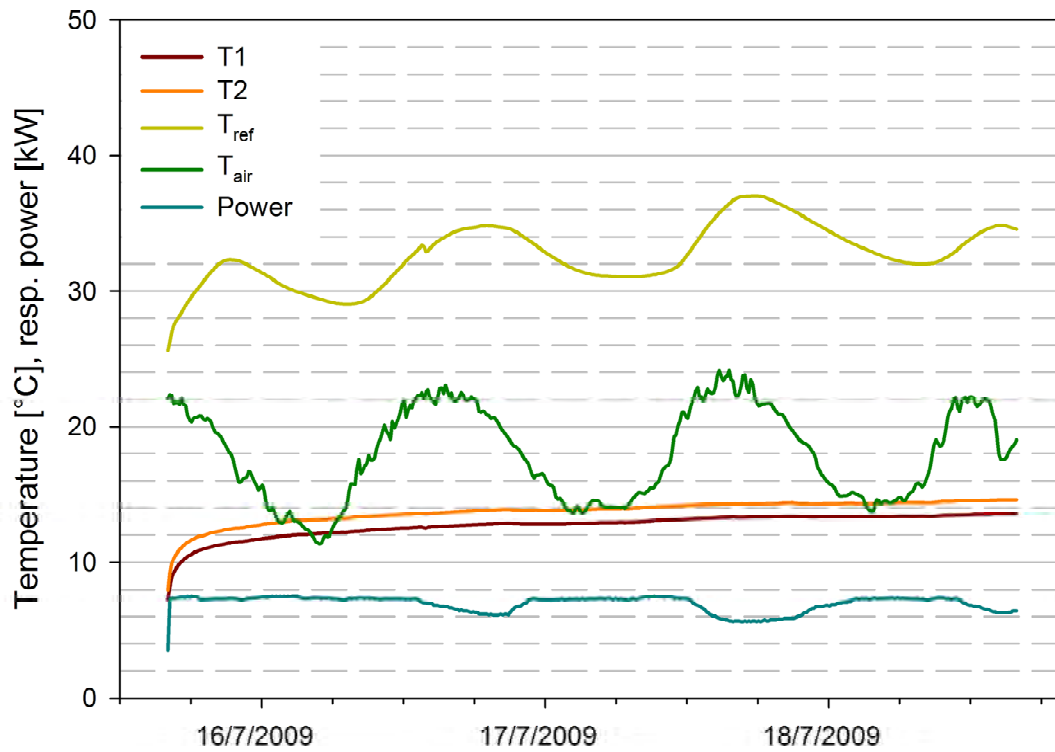


Fig. A13: TRT at Smestad. T1: up-flow temperature, T2: down-flow temperature, T_{ref} : reference temperature inside the TRT trailer, T_{air} : ambient air temperature, Power: used for the heat elements and the circulation pump.

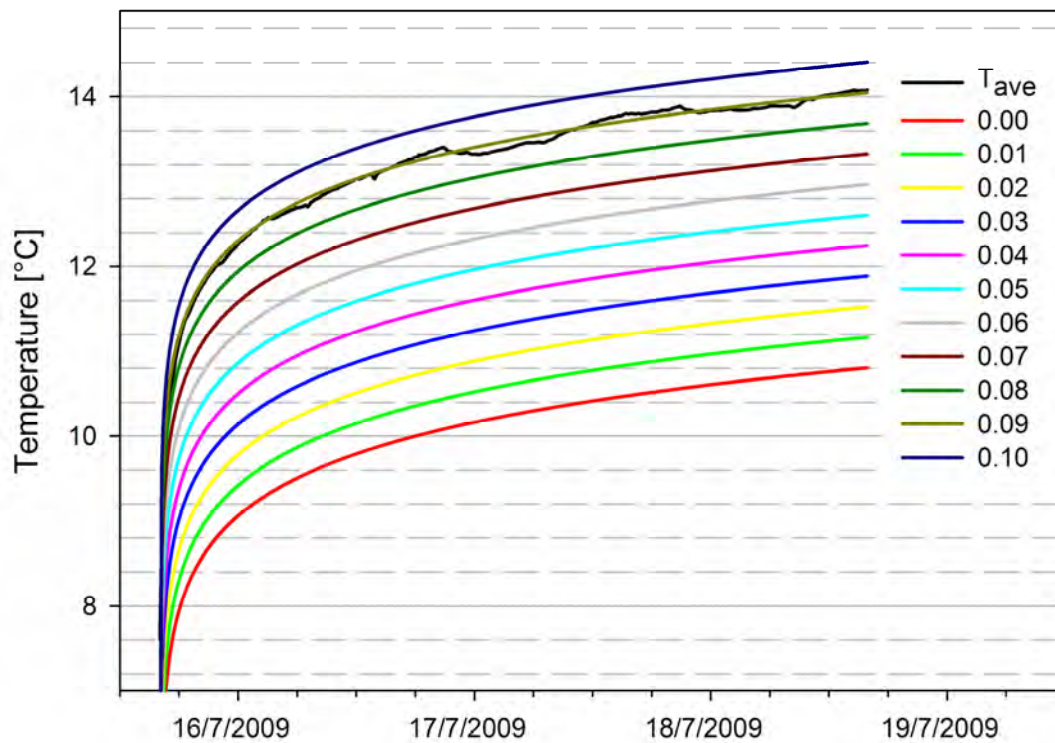


Fig. A14: Average fluid temperature in the collector (T_{ave}) and borehole resistance type curves [$K m W^{-1}$] at Smestad.

APPENDIX B: Borehole resistance, Bryn

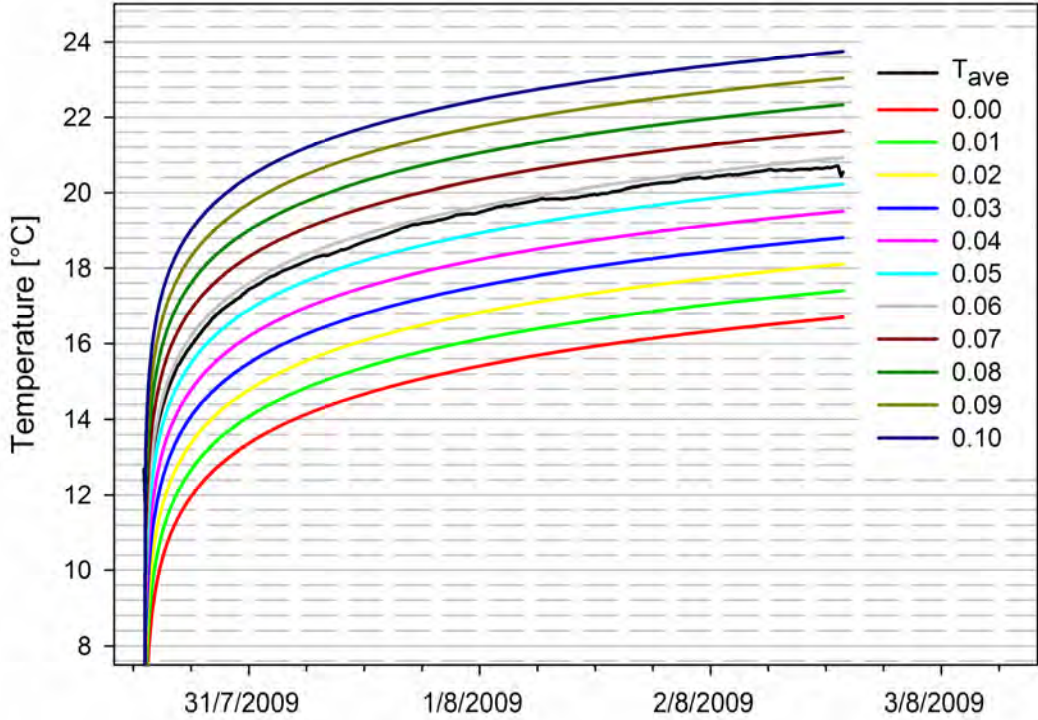


Fig. B1: Average fluid temperature in the collector (T_{ave}) and borehole resistance type curves [$K m W^{-1}$] at Bryn during TRT2 (without pumping of groundwater).

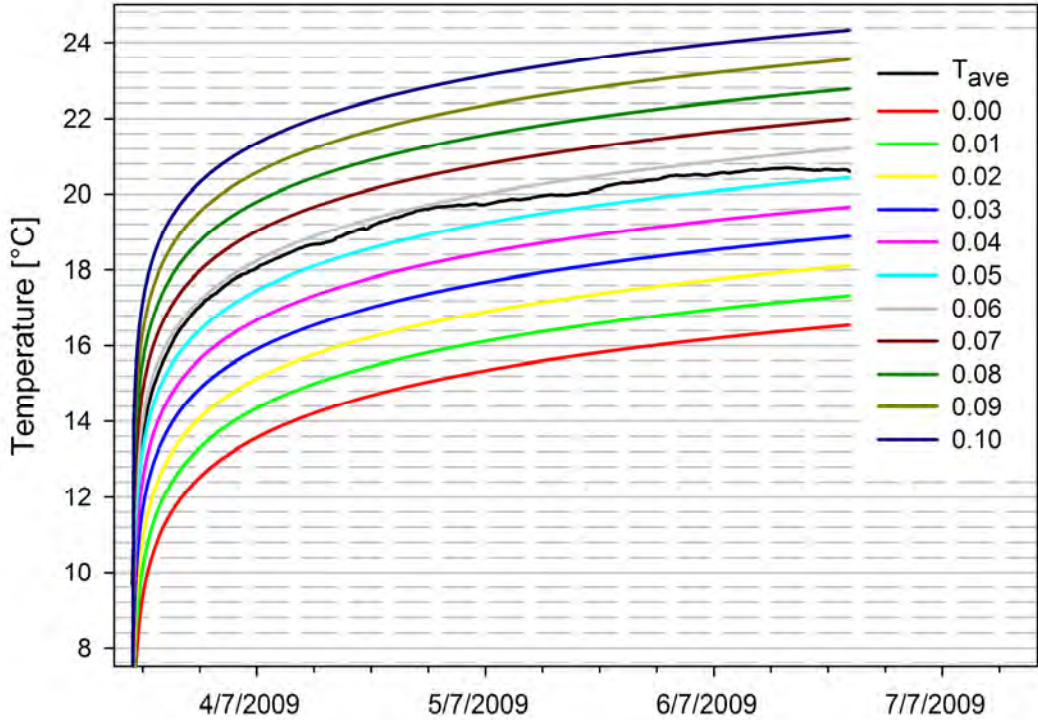


Fig. B2: Average fluid temperature in the collector (T_{ave}) and borehole resistance type curves [$K m W^{-1}$] at Bryn during TRT1 (with pumping of groundwater).